Earth Surface Dynamics
Open Access

Discussions

EGU

Reconstruction of North American drainage basins and river discharge since the Last Glacial Maximum

Andrew D. Wickert[1]

[1]Department of Earth Sciences and Saint Anthony Falls Laboratory, University of Minnesota,
Minneapolis, MN, USA

Correspondence to: A. D. Wickert (awickert@umn.edu)

Abstract. Over the last glacial cycle, ice sheets and the resultant glacial isostatic adjustment (GIA)
rearranged river systems. As these riverine threads that tied the ice sheets to the sea were stretched,
severed, and restructured, they also shrank and swelled with the pulse of meltwater inputs and time-
varying drainage basin areas, and sometimes delivered enough meltwater to the oceans in the right

5   places to influence global climate. Here I present a general method to compute past river flow paths,
drainage basin geometries, and river discharges, by combining models of past ice-sheets, glacial iso-
static adjustment, and climate. The result is a time series of synthetic paleohydrographs and drainage
basin maps from the Last Glacial Maximum to present for five published models of the North Amer-
ican ice sheets. I compare these maps with drainage reconstructions based purely on field data, such

10 as river deposits and terraces, isotopic records, mineral provenance markers, glacial moraine histo-
ries, and evidence of ice-stream and esker flow directions. The sharp boundaries of the reconstructed
past drainage basins complement the flexurally-smoothed GIA signal more often used to validate ice-
sheet reconstructions, and provide a complementary framework to reduce nonuniqueness in model
reconstructions of the North American ice sheet complex.

15 ## 1   Introduction

At the time of Last Glacial Maximum ice extent, ca. 30 ka to 19.5 ka (Clark et al., 2009; Lambeck
et al., 2014), North American drainage configurations and river discharge were dramatically dif-
ferent from present. Ice advance rerouted rivers (e.g., Ridge, 1997; Curry, 1998; Blumentritt et al.,
2009), and ice streams fed temporarily-enlarged drainage basins (Dyke and Prest, 1987; Patterson,

20 1998; Margold et al., 2014, 2015). The growth of the ice-sheets changed atmospheric circulation by
generating up to ∼4 km of high-albedo ice-surface topography (Kutzbach and Wright, 1985; Ull-
man et al., 2014) that influenced global climate and therefore patterns of drainage-basin-scale water
balance and river discharge to the oceans.

    Reconstructions of past ice-sheet thickness have proliferated (e.g., Tushingham and Peltier, 1991;

25 Lambeck et al., 2002; Peltier, 2004; Tarasov and Peltier, 2006; Tarasov et al., 2012; Gregoire et al.,
2012; Argus et al., 2014; Peltier et al., 2015), but are evaluated using limited (Tarasov and Peltier,

2006) to no (all others) geologic evidence for past drainage patterns. Instead, they are tested against terminal moraine positions and glacial isostatic adjustment, with the latter being a response that is spread across hundreds of to ~1000 kilometers due to the high flexural rigidity of the lithosphere, es-
30   pecially in the Canadian Shield provence that was covered by the ice-sheet (Kirby and Swain, 2009; Tesauro et al., 2012). Flow-routing calculations (e.g., Metz et al., 2011; Schwanghart and Scherler, 2014) are deterministic and can be used to produce time-series of drainage pathways predicted by each reconstructed ice-sheet and its associated glacial isostatic adjustment (GIA) history, forming the necessary links between the reconstructed ice-sheet and measurable geomorphic and sedimen-
35   tary records. Furthermore, the discrete boundaries of drainage basins are sensitive to ice geometry in a way that is distinct from the broad GIA response, and therefore can provide a partly-independent check on the accuracy of any given ice-sheet reconstruction (Wickert et al., 2013).

On a global scale, climate change during deglaciation may have been profoundly affected by melt-water delivery to the oceans, especially at the time of the Younger Dryas (e.g., Broecker et al., 1989),
40   but is highly sensitive to the locations of meltwater inputs to the oceans (e.g., Tarasov and Peltier, 2005; Murton et al., 2010; Condron and Winsor, 2012). Geologic data provide a timeline of meltwa-ter delivery to one basin or another (e.g., Ridge, 1997; Knox, 2007; Rittenour et al., 2007; Murton et al., 2010; Williams et al., 2012; Breckenridge, 2015), but do not provide estimates of volume. Furthermore, the relationships between geological data in different parts of the continent must be
45   connected by conservation of ice-sheet mass and glaciological continuity of ice flow. Continental-scale meltwater routing calculations that connect data and models address both of these concerns by using quantified ice-sheet thickness and ensuring that water that is not sent to one basin is sent to another, in essence serving as a "connective tissue" to ensure quantitative self-consistency.

In general, there exists a lack of recognition of the importance of Pleistocene drainage rearrange-
50   ment on river systems. In spite of the broad recognition that river systems and drainage basins have changed significantly since the LGM (Dyke and Prest, 1987; Wright, 1987; Teller, 1990a, b; Mar-shall and Clarke, 1999; Patterson, 1997, 1998; Licciardi et al., 1999; Overeem et al., 2005; Tarasov and Peltier, 2006; Wickert, 2014; Margold et al., 2014, 2015), many studies do not include any well-defined picture of drainage basin evolution. This results in representations of the modern drainage
55   network wholly or partially in place of glacial-stage drainage basins (e.g., Sionneau et al., 2008; Montero-Serrano et al., 2009; Sionneau et al., 2010; Lewis and Teller, 2006; Tripsanas et al., 2007) that help to propagate a lack of consciousness about the continental-scale hydrologic changes that occurred, even in cases when the study acknowledges in the text that past drainage pathways were different. Model-based studies likewise either test a range of possible drainage basin areas (Overeem
60   et al., 2005) or assume that the rivers have remained unchanged (Roberts et al., 2012). In the former case, this can lead to less-precise calculations of sediment transport and deposition. In the latter case, this violates the underlying assumptions used to compute erosion and infer spatially-distributed up-lift. All of these scenarios highlight the need for an improved community-wide understanding of the

ice-age effects on the continental-scale river systems of North America that provides the necessary

65 backdrop to understand the present-day rivers, their origins, and their evolution.

Here, I focus primarily on nine North American river basins. These are (counterclockwise from North) the Mackenzie River (*Dene*, Deh Cho), Columbia River, Colorado River, Rio Grande (*Es.*, Río Bravo), Mississippi River, Susquehanna River, Hudson River (*Lenape*, Muhheakantuck; *Iroquois*, Muh-he-kun-ne-tuk), Saint Lawrence River (*Fr.*, Fleuve Saint-Laurent; *Tuscarora*, Kahnawá'kye,

70 and Hudson Bay/Hudson Strait (*Inuktitut*: Kangiqsualuk ilua). These rivers span a north–south gradient of catchments that were dramatically and directly impacted by Quaternary glaciation and those that were far from the ice sheet, and together constitute a reasonably representative set of rivers from which the continental-scale hydrologic impact of glaciation on North American drainage basins can be surmised.

75 The present work is inspired by the dual and connected needs for (1) an appropriate mapping tool for data–model intercomparison, and (2) maps of the past drainage basins of North America to inform geologic studies. I first present a standardized and automated method to extract past drainage pathways and river discharges from combinations of ice-sheet, GIA (Mitrovica and Milne, 2003; Kendall et al., 2005), and climate (Liu et al., 2009; He, 2011) reconstructions. I then apply this

80 method to four ice-sheet models: the old but still-relevant ICE-3G (Tushingham and Peltier, 1991); the "industry standard" ICE-5G (Peltier, 2004); the ANU model, developed by a separate research group (Lambeck et al., 2002), the ice-physics-based "G12" model (Gregoire et al., 2012), and the new ICE-6G (Argus et al., 2014; Peltier et al., 2015). I then compare the resultant drainage basin evolution and synthetic paleohydrographs against onshore and offshore geologic data, including

85 data-driven reconstructions of North American drainage basins.

2   Methods: Automated Drainage Reconstruction

River systems in North America have responded to synchronous and linked changes in climate, ice extent, and sea level, with the latter including GIA-induced variability. Addressing this connected climate–ice–solid-Earth system is necessary to accurately reconstruct drainage. Ice advances and

90 retreats blocked drainage pathways and rerouted rivers (Tight, 1903; Ver Steeg, 1946; Bluemle, 1972; Teller, 1973; Teller et al., 2002; Carlson and Clark, 2012; Prince and Spotila, 2013). Ice-sheet retreat left behind large isostatic depressions that held proglacial lakes, such as the massive Glacial Lake Agassiz (e.g., Breckenridge, 2015), and strongly affected drainage patterns (e.g, Fisher and Souch, 1998). Even the subtle (∼20–60 m) forebulges of continental ice-sheets have been hypothesized to

95 play major roles in drainage rearrangement (Anderson, 1988). This is especially true of the generally low-relief North American cratonal interior, where ice-sheets and GIA have been significant drivers of large-scale topographic slopes.

The drainage basin and paleohydrologic reconstructions are a combination of four inputs: (1) a digital elevation model (DEM) with high enough resolution to resolve the valleys of major river systems, (2) a prescribed ice-sheet history, (3) a model of the GIA response to that ice history, and (4) a past water balance based on general circulation model (GCM) outputs that have been offset to fit modern data at the present time step (Fig. 1. These factors together allow us to generate synthetic river discharge histories that can be compared with geologic data.

This analysis produced three major end products. The first is a spatially-distributed map of estimated mean river discharges since the Last Glacial Maximum. The second is a gridded product of river discharges to the sea, designed for coupling with general circulation models to investigate the feedbacks between ice melt, ocean circulation, and climate (see Ivanović et al., 2014). The third is a set of major drainage basin extents and a time-series of their discharges into the ocean.

The drainage analyses were performed using GRASS GIS (Neteler et al., 2012; GRASS Development Team, 2012), a free and open-source GIS software that has efficient data management, computational, and hydrologic tools. GRASS GIS is fully scriptable using a number of languages. The Python source code for these analyses has been released under the GNU General Public License (GPL) version 3 and is made available to the public at the University of Minnesota Earth-surface GitHub organizational repository, at https://github.com/umn-earth-surface/ice-age-rivers.
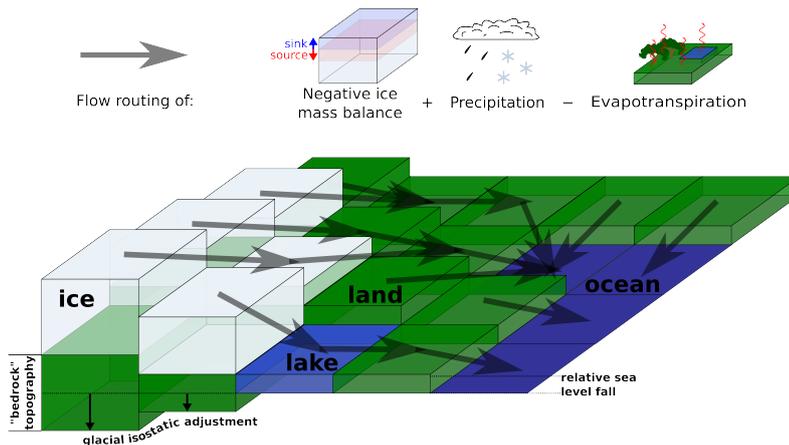
Figure 1. Meltwater and meteoric (precipitation minus evapotranspiration) water are routed to the coast, across a surface formed by the sum of present-day topography, glacial isostatic adjustment, and ice sheet thickness.

2.1 Surface elevations for flow-routing

Water and ice flow downslope following a routing surface, Z_r, that is given by:

$$Z_r = Z_{m,b} + H_i + \Delta Z_b \tag{1}$$

Z_b is the reference (i.e., modern) land-surface elevation (subscript "b" stands for "modern glacier bed" or "modern bare (i.e., ice-free) ground"), H_i is the ice thickness, and ΔZ_b represents changes between the past and modern land-surface (glacier-bed) elevation. Together, $Z_b + \Delta Z_b$ give the contemporaneous glacier bed elevation field. When this $(Z_{m,b} + \Delta Z_b)$ surface is summed with ice thickness, H_i, the resulting routing surface, Z_r, combines ice-free land-surface elevations and the elevations of the surface of the ice-sheet. This ice-sheet surface is chosen to drive the flow-routing calculations because this is what drives ice flow (cf. Cuffey and Paterson, 2010), and therefore sets ice divides and meltwater pathways. If one wanted to compute subglacial water routing instead, an alternate approach is to drive flow by the subglacial pressure gradient to simulate meltwater routing through subglacial streams and tunnel channels (e.g., Wright, 1973), and this could be accomplished by multiplying H_i by ρ_i/ρ_w, where the latter are the densities of ice and water, respectively (e.g., Livingstone et al., 2015).

2.1.1 DEM and grid resolution

Z_b is modern land-surface elevation. The primary modern elevation data set for flow routing is the GEBCO_08 30-arcsecond DEM (British Oceanographic Data Centre (BaODC) and General Bathymetric Chart of the Oceans (GEBCO), 2010). GEBCO provides the highest resolution combined topography and bathymetry data sets currently available. 30 arcseconds corresponds to a North–South cell size of 927 m, and a East–West cell size that ranges from 895 m at 15°N, the southern extent of the analysis region, to 81 m at 85°N, the northern extent. The GEBCO_08 grid is used in all areas except beneath the Greenland Ice Sheet, where the subglacial topography is interpolated from the etopo1 1-arcminute global topographic data set (Amante and Eakins, 2009).

This sub-kilometer resolution over the ice-free Earth is required to resolve flow inside the km-scale valleys of the major rivers that drain North America, and is therefore critical to accurately calculate river networks. More coarsely-gridded drainage routing can send water from the modern Upper Missouri River basin, for example, towards the Arctic Ocean. However, even these high-resolution calculations exhibit some small deviations from mapped drainage basin extents. Examples of this, such as in the Arrowhead region of Minnesota where the Saint Louis River has progressively captured Upper Mississippi drainage (van Hise and Leith, 1911; Dean and Phillips, 2011), indicate that still-higher resolution elevation data will continue to improve flow-routing calculations near headwaters streams, a scale-dependence given by the relationship between channel geometry, river discharge, and drainage area (Leopold and Maddock, 1953).

Raster grid cell area, A_c, is a function of latitude, and this is an important conversion factor for changing scalar quantities in cells, such as ice thickness, into a measure of volume. Using the simplifying assumption that Earth is perfectly spherical,

$$A_c = (R_E \delta\theta)\left(R_E \cos\left(\theta - \frac{\pi}{2}\right)\delta\varphi\right) \tag{2}$$

Here, R_E is the mean radius of Earth, θ is again colatitude, and φ is again east-longitude (i.e., degrees east of Greenwich). $\delta\theta$ is cell north–south extent, and $\delta\varphi$ is cell east-west extent; in the simulations presented here, both of these extents equal 30 arcseconds. These areas are computed at a latitude λ corresponding to the north–south midpoint of the cell, with the implicit assumption that the cells are small enough that the north–south difference in cell size can be approximated to be linear such that a straight mean accurately represents the whole. For the GEBCO_08 30-arcsecond grid that is used here, this approximation generates errors of $<0.3\%$.

2.1.2 Ice-sheet history

H_i, ice-sheet thickness, is provided by pre-generated ice-sheet reconstructions. These are produced at a coarser resolution than the 30-arcsecond flow-routing grid, and therefore are interpolated using an iterative nearest-neighbor approach to remove stepwise discontinuities that would otherwise introduce artifacts in the flow-routing calculations.

I use five ice models, four of which were created based on geophysical data, and one of which was generated using a numerical model of ice-sheet physics. In the former, ice-sheet thickness evolution was determined by inverting for global sea level data by combining (1) the total water mass contained within the ice-sheets, causing global mean sea level fall, and (2) calculations of the GIA process, which created deviations from the mean sea level history. Most notable among these deviations is that due to postglacial rebound, which is a key indicator of the presence of major past ice-sheets. However, postglacial rebound rates are a function of both time-evolving ice-sheet thickness and solid Earth (lithosphere and mantle) rheology. That this one rate is a function of two only partly-constrained variables introduces an element of uncertainty into GIA-based inversions (Mitrovica, 1996). Ice physics, on the other hand, are sensitive to the thermal evolution of the ice-sheet, related thermomechanical effects on ice rheology, and the ice basal conditions—a large number of unknowns (Tarasov and Peltier, 2006; Cuffey and Paterson, 2010). Therefore, I investigate both types of models.

ICE-3G (Tushingham and Peltier, 1991) was one of the earliest widely-used ice-sheet reconstructions. It was constructed to constrain ice thickness as much as possible with measurements of glacial isostatic adjustment from radiocarbon-dated sea level markers. While it fails to reproduce the full magnitude of the observed LGM global sea level fall (Austermann et al., 2013; Lambeck et al., 2014), it provides a counterpoint to more recent models that include a much more massive Laurentide ice-sheet (cf. Lambeck et al., 2002; Peltier, 2004).

ICE-5G (Peltier, 2004) has been often considered the "industry standard" global ice-sheet and GIA reconstruction. It was also built by combining geological data and geophysical inversions, and is an update to ICE-3G. It contains a very thick north–south-oriented ice dome over western Canada (Argus and Peltier, 2010) that is not located where glacial geological evidence would place the Keewatin dome. This causes its meltwater discharge to the coast to fail to match isotopic records from

the Mississippi River drainage basin (Wickert et al., 2013), and in any case, seems unlikely as the
ice-sheet would slide and thin over the soft Western Interior Seaway sediments east of the Canadian
Rockies. Nevertheless, ICE-5G remains widely-used and matches many observations (Peltier, 2004).

ICE-6G (here, shorthand for ICE-6G_C) (Argus et al., 2014; Peltier et al., 2015) is the successor to
ICE-5G. It has been shown to improve agreement with present-day GIA measurements, and matches
geological evidence for the locations of the ice domes and ice-sheet outlines (Patterson, 1998; Dyke
et al., 2003; Dyke, 2004). As ICE-6G is so new, it has not been extensively tested outside of the
group that developed it (Argus and Peltier, 2010; Argus et al., 2014; Peltier et al., 2015).

Lambeck et al. (2002) developed the Australian National University (ANU) ice-sheet model, also
based on field data constraining sea level and GIA. This model differs from ICE-3G and ICE-5G in
that it was developed regionally, and these regions were later combined into a more global picture of
ice-sheet evolution.

To produce the G12 ice model, Gregoire et al. (2012) simulated North American ice-sheet evo-
lution from the LGM to present using the Glimmer community ice-sheet model (Glimmer–CISM)
(Rutt et al., 2009). Glimmer–CISM is a thermomechanical model of ice deformation and dynamics
that uses the shallow ice approximation for its driving stresses. While the shallow ice approximation
neglects higher-order (i.e., less-important) stresses, it generally closely approximates those models
that do include higher-order terms, and its computational efficiency makes it a viable option for
long-term simulations (Rutt et al., 2009), such as the Gregoire et al. (2012) LGM–present simula-
tion. One of its major features is a collapse of the ice saddle between the Laurentide and Cordilleran
Ice Sheets at ca. 11.6 ka. Geological data, on the other hand, place the major phase of saddle col-
lapse during the Bølling-Allerød warm period, ca. 14.5–12.9 ka Williams et al. (2012); Dyke et al.
(2003); Dyke (2004), and possibly beginning as early as ∼17.0 ka (John et al., 1996; Clague and
James, 2002; Carlson and Clark, 2012). While Gregoire et al. (2012) shifted their chronology to
compare their Laurentide–Cordilleran ice-saddle collapse to the geologic record of Meltwater Pulse
1A (Fairbanks, 1989; Deschamps et al., 2012), I use their model ages as direct geologic age. Most
importantly, the ice dynamics contained within Glimmer–CISM provide it a set of tools to match
reality that place it in a different category than the GIA-based models.

2.1.3 Change in land-surface elevation: glacial isostatic adjustment

ΔZ_b, change in land-surface (glacier bed) elevation, is here provided by the combination of changes
in global mean sea level (GMSL) and GIA. At the Last Glacial Maximum, GMSL was ∼135 m lower
than present, but local relative sea level was highly variable due to the effects of GIA (Lambeck et al.,
2014). GIA comprises deformational, gravitational, and rotational effects of ice-age loading. The de-
formational component is the local flexural isostatic response to changes in ice and water loading.
The gravitational component is in response to redistribution of mass (and hence, gravitational po-
tential) across the surface of Earth, and this is amplified by the water self-gravitation feedback (e.g.,

7

Mitrovica and Milne, 2003). The rotational component is also the response to changing near-surface

225 mass distributions that perturb the moment of inertia and produce true polar wander that causes the

equatorial bulge to migrate, first in the form of seawater and later in the form of solid Earth material.

These three components feed back into one another, and therefore are solved numerically through

iteration.

This gravitationally self-consistent sea level theory and its numerical implementation are de-

230 scribed by Mitrovica and Milne (2003) and Kendall et al. (2005), respectively, who calculate the

GIA effects of changing ice and water masses. The calculations are performed using a pseudo-

spectral algorithm that, for this work, is truncated at spherical harmonic degree and order 256. This

satisfies the Nyquist flexural wavenumber for the solid Earth models employed, thereby allowing the

solutions to be interpolated to an arbitrarily high resolution.

235

ICE-3G, ICE-5G, ICE-6G, and ANU were each calibrated to match sea level data based on spe-

cific 1D models of solid Earth viscoelasticity (Tushingham and Peltier, 1991; Lambeck et al., 2002;

Peltier, 2004; Argus et al., 2014; Peltier et al., 2015). I use their respective spherically symmetric

models of Earth as a Maxwell body to simulate its response to these loads—VM1 for ICE-3G, VM2

240 for ICE-5G, VM5a for ICE-6G, and an unnamed model for ANU. G12 was built using a simplified

model of isostatic response to glacial loading, and was run only for North America. I pair it with

VM2, and *a posteriori* enforce a total global ice-sheet volume (and therefore GMSL history) equal

to that of ICE-5G. Among these solid Earth models, VM5a is largely a simplification of VM2, while

the ANU solid Earth model has a higher viscosity contrast between the upper and lower mantle than

245 VM2, placing it in better agreement with geophysical inferences of the upper mantle–lower mantle

viscosity contrast based on observations of the long-wavelength geoid (Hager and Richards, 1989).

I initiate the GIA modeling of G12 in equilibrium at the LGM, and ANU slightly before the

LGM. ICE-5G includes hypothesized ice-sheet growth since 120 ka. This start point is during the

last interglacial (MIS 5e), when GMSL peaked 5.5–7.5 meters above its present level (Dutton and

250 Lambeck, 2012; Hay et al., 2014), though with some significant fluctuations (Hearty et al., 2007;

Rohling et al., 2007; Dutton and Lambeck, 2012; Hay et al., 2014). ICE-3G was initiated at the last

interglacial as well, with ice slowly grown in a simple pattern towards the LGM before starting to

shrink.

Our flow-routing calculations neglect geomorphic change for three major reasons. First, signif-

255 icant changes Lake Agassiz outflow directions occurred as a precursor to spillway incision (Teller

et al., 2002), meaning that ice-sheet geometry and GIA are the primary drivers of drainage change.

Second, while process-based landscape evolution models exist (cf. Tucker and Whipple, 2002; Will-

goose, 2005), the thresholded and highly nonlinear relationships between flow, erosion, sediment

transport, and deposition, means that these models may predict a very wide range of potential land-

260 scape responses with sufficient uncertainty as to reduce their predictive capability. This would leave

changing the DEM's by hand as an option (as was done by Tarasov and Peltier, 2005), but consid-

ering incomplete knowledge of past topography and my desire to, at least at this stage, separate the calculations from the field work against which they are checked, I choose to use modern topography while acknowledging that this is an approximation.

265 ## 2.2 Water balance: precipitation, evapotranspiration, and ice melt

Each cell in the flow-routing grid domain can act as a source of water to continental drainage systems. Water balance over each cell is a sum of precipitation gains, P, evapotranspiration losses, ET, and changes in water-equivalent thickness of the ice-sheet reconstruction, $(dH_i/dt) * (\rho_i/\rho_w)$. When multiplied by the cell area, A_c (Eq. 2), the result is an expression for volumetric incoming water

270 discharge, Q_{in} (Eq. 3).

$$Q_{\text{in}} = A_c \left(P - ET - \frac{\rho_i}{\rho_w} \frac{\Delta h_i}{\Delta t} \right) \tag{3}$$

2.2.1 Global precipitation and evapotranspiration

Precipitation and evaporation inputs changed through time (Fig. 2). These changes were calculated by Liu et al. (2009) and He (2011) using a continuous LGM (22 ka) to present run of the National

275 Center for Atmospheric Research (NCAR) Community Climate System Model version 3 (CCSM3) (Collins et al., 2006). This simulation, called TraCE-21K, was run at 3.5 degree resolution. I spherically interpolated (following Dierckx, 1993) the results to 0.25 degree (15 arcminute) resolution to match the assembled modern data products (below).

The low resolution CCSM3 contains systematic biases that produce a ∼1 mm/day positive pre-

280 cipitation anomaly in western North America and a ∼1 mm/day negative precipitation anomaly in eastern North America (Yeager et al., 2006). To correct for this and other possible model biases, I assembled modern precipitation and evapotranspiration fields, computed the difference between each time-step of TraCE-21K and its modern time-step, and summed the modern compilations with the computed TraCE-21K difference from modern. I could find no global evapotranspiration product,

285 and global precipitation products were coarse, often at 2.5-degree resolution (∼280-km cells at the equator) (Xie and Arkin, 1997; Chen et al., 2002; Adler et al., 2003). Therefore, I generated my own global data product compilations as mean rates from 2000 to 2004, for consistency with prior work (Wickert et al., 2013), at 0.25° resolution.

I derived the precipitation data by stitching together three data products. The CRU TS3.21 0.5°

290 precipitation product provided precipitation over the global continents except Antarctica (expanded from the work of Harris et al., 2014), and this was smoothed and spherically interpolated (following Dierckx, 1993) to 0.25° resolution. The HOAPS-3 satellite-derived precipitation data product (0.25° resolution) was used for the oceans north of the Antarctic region (Andersson et al., 2010). Gaps of 2° or less between these data sets were filled by an interpolation of them. The remainder of the globe,

295 primarily the Antarctic region, was filled by the CMAP reanalysis data set (Xie and Arkin, 1997), interpolated from 2.5° resolution to 0.25° resolution.

Our modern evapotranspiration rates for the continents (except Antarctica) are based on calculations using the MODerate-resolution Imaging Spectroradiometer (MODIS) instruments that are mounted on the Aqua and Terra satellites (Mu et al., 2007, 2011), available at 30-arcsecond reso-

300 lution. The oceanic evaporation data are from HOAPS-3 and at 0.25° resolution (Andersson et al., 2010). Analysis of the HOAPS-3 data product shows that it has an ∼10% error, with a global 0.2–0.5 mm day^{-1} excess evaporation (Andersson et al., 2011). These data sets were interpolated over the ice-free land surface and global oceans. Evapotranspiration rates for Greenland and Antarctica were taken from the 0-ka time step of the TraCE-21K simulation (Liu et al., 2009; He, 2011), spher-

305 ically interpolated to 0.25° resolution and thresholded at 0 to prevent the interpolation method from generating negative evapotranspiration rates.
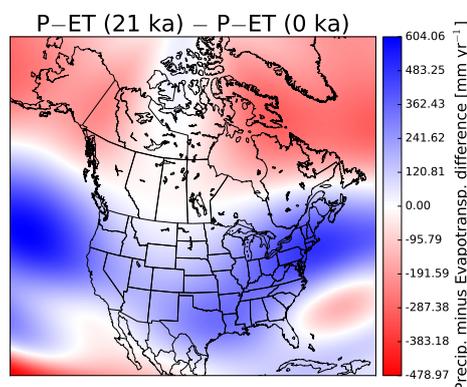
Figure 2. Modeled changes precipitation minus evapotranspiration between the Last Glacial Maximum and present. These differences were calculated with the TraCE-21K continuous LGM to present paleoclimate run (Liu et al., 2009; He, 2011) of the CCSM3 GCM (Collins et al., 2006). They are combined with ice mass balance to produce water inputs for computed paleodischarges

2.2.2 Ice melt and central differencing

Ice-sheet inputs to runoff are determined by differencing ice-sheet thicknesses at adjacent time steps for each of the ice models. These differences in ice-sheet height are converted to water discharges

310 by (1) multiplying them by the DEM cell size ($\propto \cos(\text{latitude})$), (2) multiplying them by 0.917 as a conversion factor between ice and water density, and (3) dividing them by the time elapsed (Eq. 3).

Flow routing and drainage basins can be calculated only on time steps when the ice-sheet and GIA models provide surface topography (Section 2.3, below), but the ice-sheet contribution to runoff requires ice-sheet thickness to be differenced, and thus should be most valid for the times halfway

315 between the ice thickness time-steps. This requires a choice of whether to allow numerical diffu-
sion in space (i.e., flow-routing) or time (i.e., melt rate). Melt rates change more gradually than
near-instantaneous drainage rerouting events, and these rerouting events are thought to be critical
to understanding climate impacts of ice melt (e.g., Broecker et al., 1989; Tarasov and Peltier, 2006;
Condron and Winsor, 2012). Therefore, I prefer numerical diffusion in time, and allow the gridded

320 melt rate at each ice-sheet reconstruction time-step to equal the averages of the melt rates calcu-
lated between this time step and those before and after it. This is the same as a central-difference
calculation when time-steps are uniform.
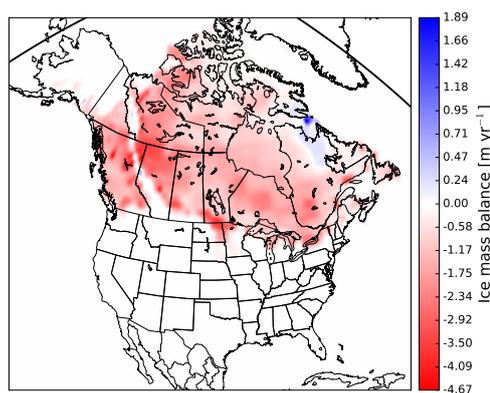
Figure 3. Ice-sheet melt is an important input to calculations of past water discharge. Ice surface mass balance
shown here is for the ICE-6G (Argus et al., 2014; Peltier et al., 2015) between 14.5 and 14.0 ka.

2.2.3 Neglected terms: groundwater and lakes

While groundwater is a significant reservoir that affects river discharge, I assume that over the

325 millennial time scales of interest to us, groundwater discharge will be in equilibrium with atmo-
spheric inputs. Although ice-sheets can strongly influence groundwater discharge, modeling work
by Lemieux et al. (2008) shows that the maximum net deglacial groundwater discharge across the
whole North American continent is only ∼2.5% the modern Mississippi River discharge, and that
this spike was short-lived.

330 I do not include proglacial lakes in the continental water storage because the ice-sheet reconstruc-
tions discussed here (Tushingham and Peltier, 1991; Lambeck et al., 2002; Peltier, 2004; Gregoire
et al., 2012; Peltier et al., 2015) do not. This means that these models implicitly include the lake-
water volume within the ice mass. This deficiency affects the ability of the models to match the ob-
served ice-sheet geometry, as ice must be used in the models to represent the surface loads of these

335 large lakes in the geologic past, and removes the potential effects of the lakes in driving ice-sheet

retreat in mechanistic models. In this work, water is simply routed across proglacial-lake-producing depressions (see Section 2.3).

2.3 Continental flow routing and accumulation

After defining the amount of flow each cell contributes to runoff, I used the time-evolving grids
340 of surface elevation to compute drainage patterns across North America. I first specified that the drainage outlets must occur along the coast at that time-step. I then routed flow down the Z_r (Eq. 1) surface while computing accumulated discharge as (1) meteoric inputs only, (2) ice-sheet inputs only, and (3) combined total discharge. I computed this flow routing and accumulation using "r.watershed", the high-efficiency least-cost path search algorithm of Metz et al. (2011), which is
345 integrated into GRASS GIS (Metz et al., 2011; Neteler et al., 2012; GRASS Development Team, 2012).

2.3.1 Defining continent, ocean, and shore

Shorelines and topographic elevations changed dramatically since the Last Glacial Maximum, thus requiring redefinition of the coastline on which river mouths appear at each time-step. This could not
350 be done by simply picking regions below sea-level, because this approach would, for example, cause flow to "disappear" into the below-sea-level Caribou Basin of Lake Superior and/or into regions around the ice margin that were isostatically depressed below sea-level. Therefore, I developed an algorithm to define as "ocean" only those regions that were below sea-level and contiguous with the global ocean. First, I thresholded the topography-plus-ice flow-routing map, Z_r, at 0, to define a
355 binary raster map. Then, I converted this into a vector map. Using the topological analysis built into GRASS GIS, I looked only for areas that touched the map edge, and chose these to be ocean. The remaining area was defined as continent and used as the flow-routing surface.

2.3.2 Flow routing and accumulation

Our flow-routing calculations produce maps of (1) drainage direction, (2) meteoric water discharge,
360 (3) meltwater discharge, and (4) total water discharge. These maps are spatially-distributed, providing 30-arcsecond-resolution time-series of the time-averaged surface water discharge that is produced by each ice-model–solid-Earth-model combination.

The flow-routing algorithm I used, r.watershed (Metz et al., 2011), uses a least-cost path search algorithm that sets it apart from other drainage analyses in that it is capable of routing water through
365 depressions without explicitly flooding them (see, e.g., Schwanghart and Scherler, 2014). This algorithm allows for rapid calculations to be carried out over a landscape that contains moving ice dams and isostatic depressions.

While it is essential to ignore local depressions in the DEM and properly reconstruct the full length of drainage systems through the shifting proglacial lakes of the Late Quaternary North America, it

370　causes internally drained regions to be amalgamated to drainage basins that flow to the coast. In the
drainage calculations performed for this work, the Great Basin remains split between the Colorado
River and Columbia River drainage basins. In part, this is realistic: outflow from Lake Bonneville
entered Columbia River between 18.2±0.3 ka (McGee et al., 2012) and ∼17.5–17.4 ka (∼14.4–14.3
^{14}C ka; calibrated with IntCal13 Reimer et al., 2013) (Godsey et al., 2005), with a massive <1-year

375　flood from Lake Bonneville ending this period of inter-basin interchange. In part, a hydrologically-
closed basin must maintain a state in which precipitation equals evapotranspiration, and as such
should not have a major effect on discharge calculations, outside of the aforementioned period of
climate change during the end of the Pleistocene. But in part, this is the dissatisfying result of flow-
routing calculations that are not coupled to a hydrologic model that can raise and lower the levels of

380　lakes in closed basins, and a fundamental problem of any approach that disconnects local hydrologic
balances and flow-routing.

　　This dilemma over the Great Basin highlights a key question in how much to adjust the model
by hand to fit data, versus how much to just allow the model to run. It would be possible to modify
the flow-routing inputs to declare the Great Basin to be closed throughout part or all of the modeled

385　geologic past. The approach taken here is to leave the flow-routing grid unmodified in order to
maintain distance between data and model (see the final paragraph in Section 2.1.3).

2.4　Distributed melt delivery to the coast

These methods also allow us to produce grids of meltwater discharge to the coast that are fully-
distributed in space and time. These have been converted to GCM-input-appropriate spatial reso-

390　lutions and used in preliminary work to connect ice melt and global ocean circulation and climate
change (Ivanović et al., 2014). This is an improvement over "hosing" experiments (e.g., Condron
and Winsor, 2012), which have thus far been central to any model-based understanding of melt-
water impacts on climate change. In "hosing" experiments, meltwater additions are prescribed to a
patch of ocean. The fully-distributed GCM meltwater inputs create a more realistic ice-age ocean

395　that is better-conditioned to respond to changes in meltwater inputs (that again, are distributed),
and can be used to connect models of ice-sheet history with their likely impacts on global climate.
Code to produce these GCM inputs is also provided in the Github repository (https://github.com/
umn-earth-surface/ice-age-rivers).

2.5　Drainage basins and river discharge

400　I compute time-evolving drainage patterns with a generalized algorithm that can overcome changes
in shoreline geometry, river mouth positions, and difficulties in consistent topography-based flow
reconstruction across the very subtle topography of the continental margins. These components are
essential to connect glacial-stage rivers to their modern counterparts after 20,000 years of shoreline
and topographic change due to evolving sea level and ice-sheet geometry.
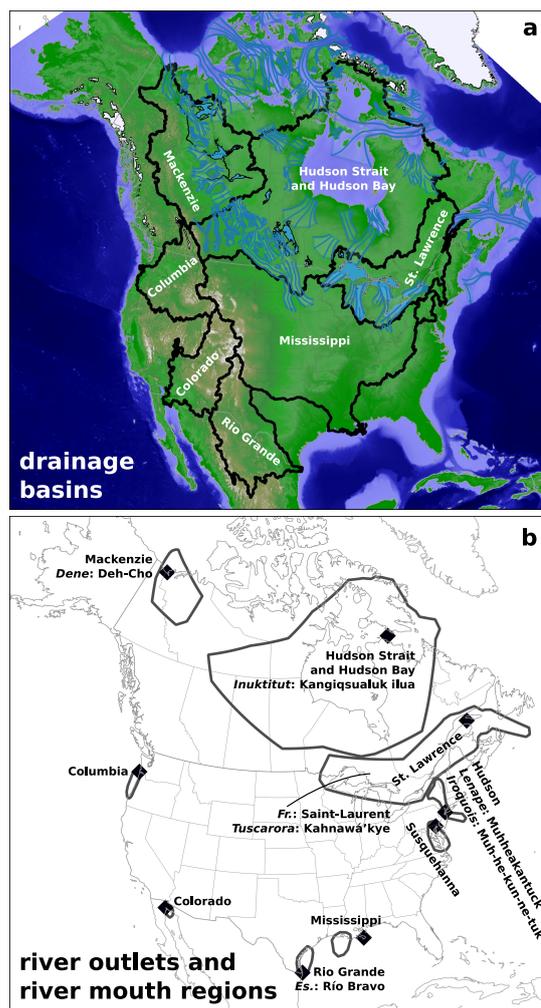
Figure 4. a. Modern drainage basin extents for the rivers involved in this study, with ice and lake extents from the 1 ka time-step of the maps of Dyke (2004), elevation basemap from British Oceanographic Data Centre (BaODC) and General Bathymetric Chart of the Oceans (GEBCO) (2010), and modern drainage basins from Lehner et al. (2013). **b.** Modern river mouths alongside the river mouth regions used to define a flow path as part of a drainage basin (Section 2.5). Names are also given in European non-English languages where they are common, alongside a non-exhaustive set of common names in local languages. Note that the mouth of the Mississippi River lies entirely outside its river mouth region. This is because the topographically-routed flow (Metz et al., 2011) follows the course of the Atchafalaya River; the present course of the Mississippi runs counter to the regional topographic gradient because it is held in its old course by the Old River Control Structure (e.g., Harmar and Clifford, 2007).

First, I create a map of regions where I expect the mouth(s) of each river system to be. Each "river mouth region" (Fig. 4b) is defined by hand to accommodate the changing locations of river mouths with time as a function of sea level, ice cover, and GIA (Figure 5. This is especially important for drainage systems such as Hudson Strait and the Saint Lawrence River, which previously played host to ice streams and now are fully or partially inundated with seawater.

I then create a set of points at which each of the "major" rivers (≥ 1000 m^3 s^{-1} reconstructed discharge) reaches the coast. Wherever one of these river mouths is located inside a named region (Fig. 4), I build a drainage basin. Each drainage basin is labeled with the name of its respective river mouth region (e.g., "Mississippi" or "Columbia"). River mouth regions that contain more than one river mouth produce a named drainage basin that is an amalgamation of the drainage basins of all ≥ 1000 m^3 s^{-1} rivers in the basin; this allows us, for example, to combine the Mississippi, Atchafalaya, and Red Rivers into a single broader basin flowing towards Louisiana, and to combine all of the major modern rivers that flow into Hudson Bay into a single basin, even though their previous combined outlet in Hudson Strait is now inundated. If a particular river mouth region contains no river mouths with flow ≥ 1000 m^3 s^{-1}, I build a drainage basin based on the highest-discharge coastal cell from the flow accumulation calculation.

After defining the major drainage basins, I sum (1) ice-sheet melt, (2) precipitation minus evapotranspiration, and (3) the sum of (1) and (2) across each basin. Each sum, respectively, provides ice-sheet meltwater discharge (Q_i), meteoric (seasonal precipitation minus evapotranspiration) discharge (Q_m), and total river discharge ($Q = Q_m + Q_i$). Many of these calculations provide discharges at the modern time-step that are close to the modern pre-human-impact mean river discharge (Table 1, which also includes sediment discharges for reference) For some, however, the result differs somewhat due either to (1) the water balance maps not perfectly representing water delivery to the coast and/or (2) the incorporation of the internally-drained Great Basin into the Columbia River and Colorado River basins because the flow-routing algorithm (Metz et al., 2011) was set up to disallow internal drainage. To provide more realistic discharge histories while also being explicit about the raw outputs of the model, I rescaled discharge in each basin to match its modern value with the mean of the computed time-steps between 3 ka and present, while also making note on the plots (Figs. 10–15) of the predicted uncorrected modern discharge. This correction may create a systematic underestimate of Columbia River discharge from 18.2±0.3 ka (McGee et al., 2012) to ~17.5–17.4 ka (Godsey et al., 2005; Reimer et al., 2013), when waters from Lake Bonneville—part of the Great Basin—flowed into the Columbia River Basin.

3 Methods: Data-driven Drainage Reconstruction

A set of entirely data-driven drainage histories provides a necessary counterpoint to evaluate the model-based computed drainage basins and river discharge histories. I developed these in two differ-
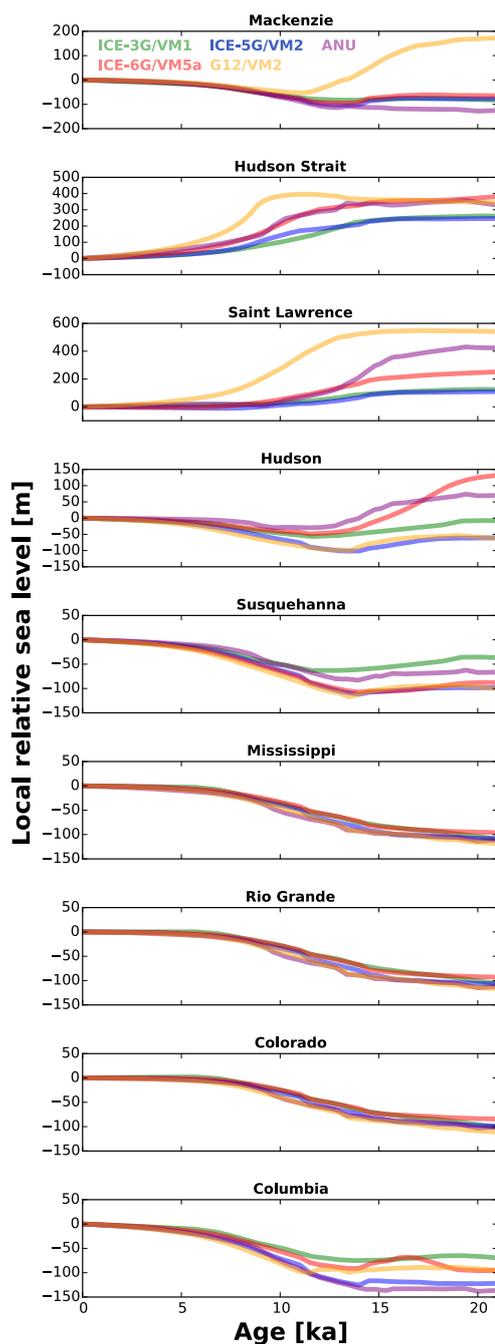
Figure 5. Sea level curves extracted from GIA models at the modern locations for the river mouths that are important to this study (Fig. 4). Wide variability highlights the different histories experienced by rivers formerly near (or under) thick ice, and those far from it.

Table 1. Modern drainage basin areas and water (Q_w) [cubic meters per second] and sediment (Q_s) [10^6 metric tons per year] discharges. Many of these were gathered and independently of the Milliman and Farnsworth (2013) compilation, and generally provide good agreement with their numbers.

River	A [km^2]	Q_w [m^3 s^{-1}]	Q_s [Mt yr^{-1}]	Reference(s)
Mackenzie	1.8×10^6	9910	128	Carson et al. (1998)
Hudson Strait and Bay	1.173×10^6	$30,900^a$	$\sim 1.1^{a,b}$	Schneider-Vieira et al. (1994); Bentley (2006)
Saint Lawrence[c]	$1.344 \times 10^{6[d]}$; $1.61 \times 10^{6[e]}$	$12,000^d$; $14,400^e$	3.6^d	Holeman (1968); Doyon (1996); Dolgopolova and Isupova (2011); Environment Canada (2013)
Hudson River	0.034×10^6	590	0.737	Wall et al. (2008); Milliman and Farnsworth (2013)
Susquehanna	0.0704×10^6	1082	5	Gross et al. (1978); Kammerer (1990)
Mississippi[f]	3.225×10^6	$18,430^f$	400^g, 210^i	Kammerer (1990); Milliman and Farnsworth (2013)
Rio Grande	0.870×10^6	$570^{g,h}$; 22^i	$20^{g,h}$; 0.66^i	Gates et al. (2000); Milliman and Farnsworth (2013)
Colorado[j]	0.637×10^6	$\sim 665^{g,h}$; 6.3^i	$145^{g,h}$, 0.1^i	U.S. Bureau of Reclamation (1952); van Andel (1964) (as cited by Carriquiry and Sánchez, 1999); Kammerer (1990); Prairie and Callejo (2005); Nowak (2011); Milliman and Farnsworth (2013)
Columbia	0.668×10^6	7500	7	Milliman and Meade (1983); Kammerer (1990)

[a] This is the sum of river inputs to Hudson Bay from pre-1975 data

[b] Modeled following Syvitski et al. (2003)

[c] Not including modern diversions into or out of the Great Lakes. These include the Chicago Diversion (out of the Great Lakes basin), and the Ogoki and Long Lake Diversions (into the Great Lakes basin). The drainage basin figures show the modern Great Lakes basin, but as these diversions are small compared to other sources of possible error, I have not returned the mapped drainage basin to its pre-diversion state.

[d] The Great Lakes–Saint Lawrence drainage system alone

[e] Including inflow into the Saint Lawrence estuary from rivers other than the Saint Lawrence

[f] This is the sum of Mississippi River (Old River) discharge and drainage area, and Mississippi River discharge and drainage area routed towards the Atchafalaya River. The addition of the Atchafalaya-Red River system increases drainage area from 2.978×10^6 km^3 to 3.225×10^6 km^2, and discharge from 16,790 m^3 s^{-1} to 18,430 m^3 s^{-1}.

[g] Before the installation of river control structures; all values (including those on the same line) are modern unless indicated

[h] Before modern water withdrawals; these values are estimated based on the work of Gates et al. (2000) for the Rio Grande and Prairie and Callejo (2005) and Nowak (2011) for the Colorado River at Imperial Dam, which was summed with inputs from the Gila River (U.S. Bureau of Reclamation, 1952); see Cohen et al. (2001) for an earlier calculation of natural discharge to the Colorado River delta, and Schmidt et al. (2010) for a review of the 20th century human–river interaction that necessitated my approximation here. Modern values of water and sediment discharge are from Milliman and Farnsworth (2013).

[i] Modern discharge to the ocean.

[j] Modern discharge values are from Milliman and Farnsworth (2013); past estimates and the estimated sediment yield are from other sources.

440　ent ways: as paleogeographic maps of drainage divide positions, and as a categorical river discharge
history that defines periods of high and low flow.

　　I developed a set of data-driven drainage basin boundaries for each of the study basins (Figs.
6–9, lower right panels) based on several lines of evidence. The first is the modern drainage basin
outlines of Lehner et al. (2013). The second is the ice-sheet margin chronology of Dyke et al. (2003);
445　Dyke (2004), which, when lacking independent information, I use as an approximate set of contours
of ice-sheet thickness. The ice divide could, however, have moved with time, offsetting it from
the chronological contours. Therefore, a key third set of information comes from the evidence of
ice streaming recently completed by Margold et al. (2014, 2015) and the mapped Canadian eskers
from Storrar et al. (2013). As there are few chronological controls on when these ice-streams were
450　active, ice divides are drawn between diverging ice-streams. This may not be such a bad assumption:
where there are chronological controls on ice-stream reorganization, the changes in drainage tend to
produce modest and localized changes in catchment area and/or outlet location (e.g., Stokes et al.,
2009; Ross et al., 2009; Ó Cofaigh et al., 2010). Better chronologies often come from direct dating
of ice-marginal positions (e.g., Licciardi et al., 1999; Dyke, 2004; Gowan, 2013), fluvial deposits
455　(e.g., Bretz, 1969; Atwater, 1984; Ridge, 1997; Benito and O'Connor, 2003; Knox, 2007; Rittenour
et al., 2007), and lacustrine deposits (e.g., Antevs, 1922; Kehew et al., 1994; Rayburn et al., 2005,
2007, 2011; Richard et al., 2005; Breckenridge, 2007; Breckenridge et al., 2012) and these provide
the fourth layer to define drainage chronologies. The fifth layer of data comes from the offshore
stratigraphic record (e.g., Andrews and Tedesco, 1992; Andrews et al., 1999; Flower et al., 2004;
460　Carlson et al., 2007; Williams et al., 2012; Maccali et al., 2013), which can be compiled into a
paleohydrograph that may correlate with drainage basin area (Wickert et al., 2013), but does not
independently indicate where the past drainage basin margins lie.

　　While very detailed and well-dated geological constraints permit a quantitative approach to re-
construct past discharge, many are much more basic, simply showing when periods of high or low
465　discharge may have existed due to changes in drainage basin area (e.g., Ridge, 1997), isotopic ratios
(e.g., Andrews and Dunhill, 2004), and/or proglacial lake outlets (e.g., Teller and Leverington, 2004,
and later revisions). I therefore first took the simplest approach to these records, defining them as
simply "high discharge" (light and dark gray on Figs. 10–15) or "low discharge" Figs. (10–15). Dark
gray indicates times for which there is geological evidence for a distinct period high flow, and light
470　gray indicates the time over which data-based inferences indicate that enhanced flow would have
occurred and/or when discharge would have been higher but not as high as during the time indicated
by the dark gray regions. For example, Mississippi River discharge increased when Lake Agassiz
flooded into it (dark gray), but was overall higher than present from the LGM until ~12.9 ka due to
ice-sheet input and a larger drainage basin area (light gray).

4 Results

The result of the computational work is two major products: synthetic drainage basin and discharge histories. The former are summarized in four sets of maps of significant points in time since the Last Glacial Maximum (Figs. 6–9). The latter are a set of reconstructed deglacial water discharges by drainage basin (Figs. 10–15). These provide a spatially-distributed and quantified view of how rivers in North America have broadly changed over the past 20,000 years.

The counterpart to these computed histories are those that are driven by more direct interpretations of the data. I write, "counterpart" as opposed to "ground-truth" because these are also to some extent interpretations, based on limited data. Their key utility is that they offer a much simpler path from the raw data to the interpreted drainage basin extents and periods of high discharge, and one that can be more closely tied to geological fact. As such, disagreements between these data-derived basins and those derived from models, especially where the data-driven drainage basins are tightly-constrained, most likely indicate where the models should be improved.

5 Discussion

5.1 Comparison with geologic evidence for varying drainage basin areas and discharge

Each of the river systems in this study experienced high flow and low flow at different times. The high flow could be due to meltwater inputs or drainage area expansion, and often these are linked: ice-sheet advance into mid-continent drainage basins vastly increased their area (Figs. 6–8). Figure 10 includes a brief description of each of these times, and I will expand on these here with references. The data-drive drainage histories (Section 3) through North America are updated from Wickert (2014) and are broadly consistent with the work of Licciardi et al. (1999), with radiocarbon ages calibrated using IntCal13 (Reimer et al., 2013).

5.1.1 Drainage histories by river

The Mississippi, Hudson, and Susquehanna Rivers traded drainage inputs from the Great Lakes and their respective former ice lobes, resulting in a pattern of symmetric increases and decreases in discharge along the southern Laurentide margin. At the Last Glacial Maximum, the drainage area of the Great Lakes was split between the Mississippi and Susquehanna Rivers (Ridge et al., 1991; Ridge, 1997; Licciardi et al., 1999), but by 19.9 ka, ice retreat associated with the Erie Interstade rerouted southeastern Laurentide meltwater output through the Mohawk Valley in New York and towards the Hudson River (Ridge, 1997). The opening of the Mohawk Valley also rerouted flow from Lakes Erie and Ontario away from the Mississippi River and towards the Hudson River, though the deposits of the Kankakee Outwash Plain (Knox, 2007) indicates increased meltwater outflow to the Mississippi River ∼19.3–18.8 ka, with a major flood ∼19 ka (Curry et al., 2014). Following the

Earth **Surface**
Dynamics
Discussions
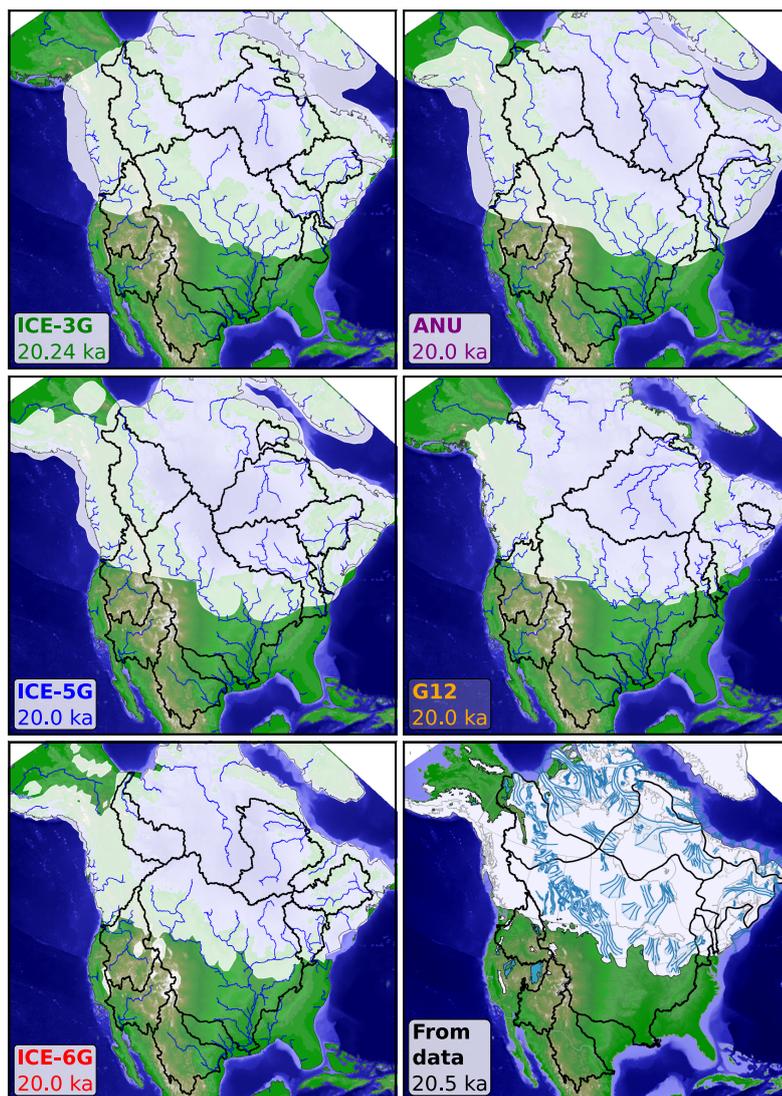
Figure 6. End of the global Last Glacial Maximum. North American drainage basins at the Last Glacial Maximum. Ice models are organized left to right, top to bottom, in the order of their publication age. Drainage basins are delimited in black. The model output plots contain blue rivers, which occur where the runoff calculations indicate streamflow that is ≥ 1000 m^3 s^{-1}. The data-driven compilation indicates evidence of past ice streams in blue (Margold et al., 2014). The model- and data-driven reconstructions show generally a consistent trend of an enlarged Mississippi River drainage basin, ice flow via Hudson Strait into the North Atlantic, and ice-sheet meltwater routed down the Hudson and/or Susquehanna Rivers.

Earth **Surface**
Dynamics
Discussions
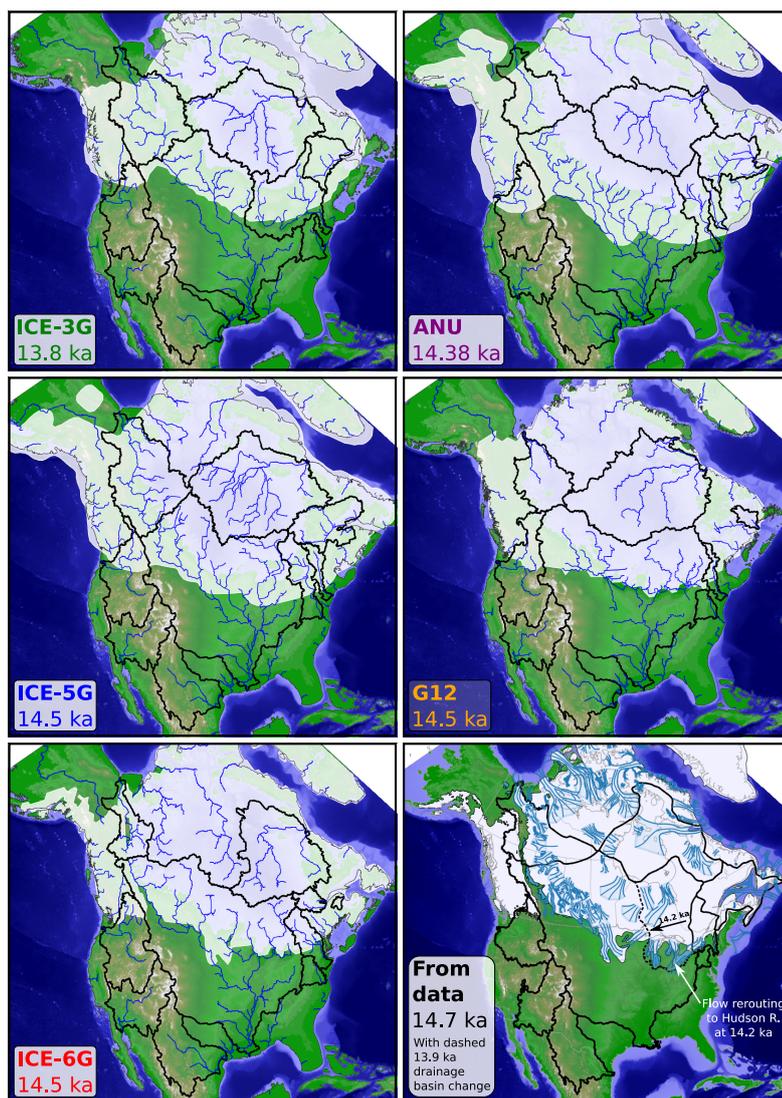
Figure 7. Bølling-Allerød warm period and (for all but ICE-3G and the data-driven reconstruction, for which the closest-available time-slice(s) was/were chosen) **Meltwater Pulse 1A.** The Bølling-Allerød warm period was the major period of warming between earlier near-LGM conditions and the later Younger Dryas cooling. The early part of the Bølling-Allerød encompasses Meltwater Pulse 1A, a period of 14–18 m sea level rise between 14.65 and 14.31 ka (Deschamps et al., 2012). Collapse of the ice saddle between the Laurentide and Cordilleran Ice Sheets at this time could be the dominant cause of Meltwater Pulse 1A (Gregoire et al., 2012). Note the expansion of the blue ≥ 1000 m^3 s^{-1} river lines for many of the ice models; this is representative of an increase in melt at this time.

Earth **Surface**
Dynamics
Discussions
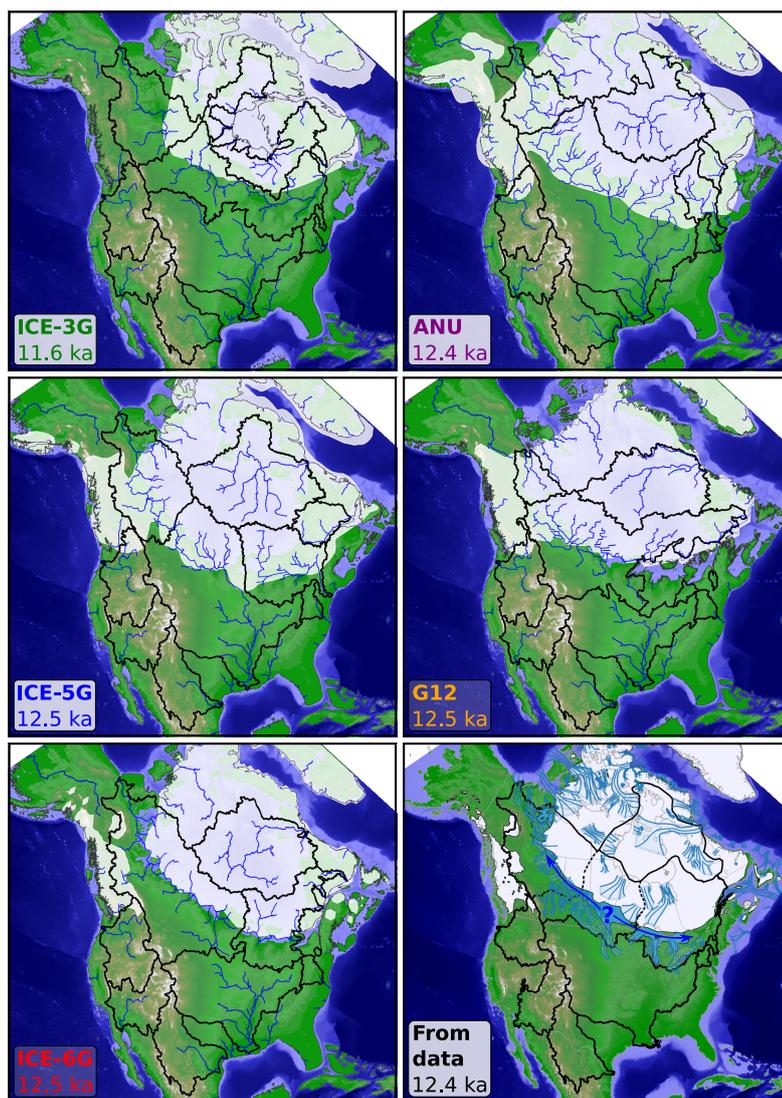
Figure 8. Younger Dryas (at transition to Holocene for ICE-3G). The Younger Dryas was a period of rapid cooling that corresponds with meltwater rerouting away from the Mississippi (Williams et al., 2012; Wickert et al., 2013) and enhanced meltwater output to the Mackenzie (Murton et al., 2010) and Saint Lawrence (Carlson et al., 2007) rivers. Model predictions here vary widely, and properly matching this continental-scale drainage rerouting away from the Mississippi basin is a feature that all successful ice models should have. The routing of flow from Lake Agassiz, at the center of the continent, was not towards the Mississippi at this time (Wickert et al., 2013), but is otherwise unclear based on current data (e.g., Carlson and Clark, 2012; Lowell et al., 2013; Breckenridge, 2015).

Earth **Surface**
Dynamics
Discussions
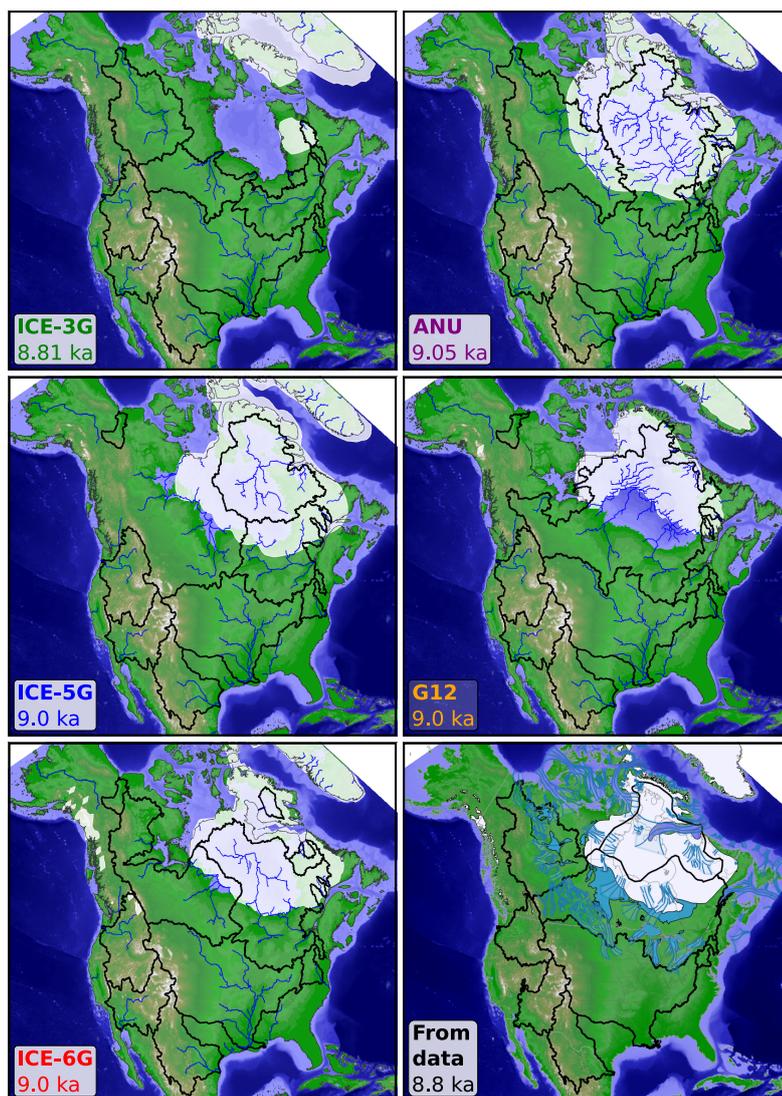
Figure 9. Early Holocene. The early Holocene was notable for its ice retreat and proglacial lake growth, which included enhanced flow down the St. Lawrence River and abrupt drainage of proglacial lakes Agassiz and Ojibway into Hudson Bay. Many other rivers no longer had ice-sheet input. In ICE-5G, the Upper Missouri river reoccupies its hypothesized preglacial channel in the Bismarck–Mandan area (Alden, 1932) and separates from the rest of the Mississippi system. This illustrates how sensitive mid-continental river systems can be to subtle tilts of the land surface.
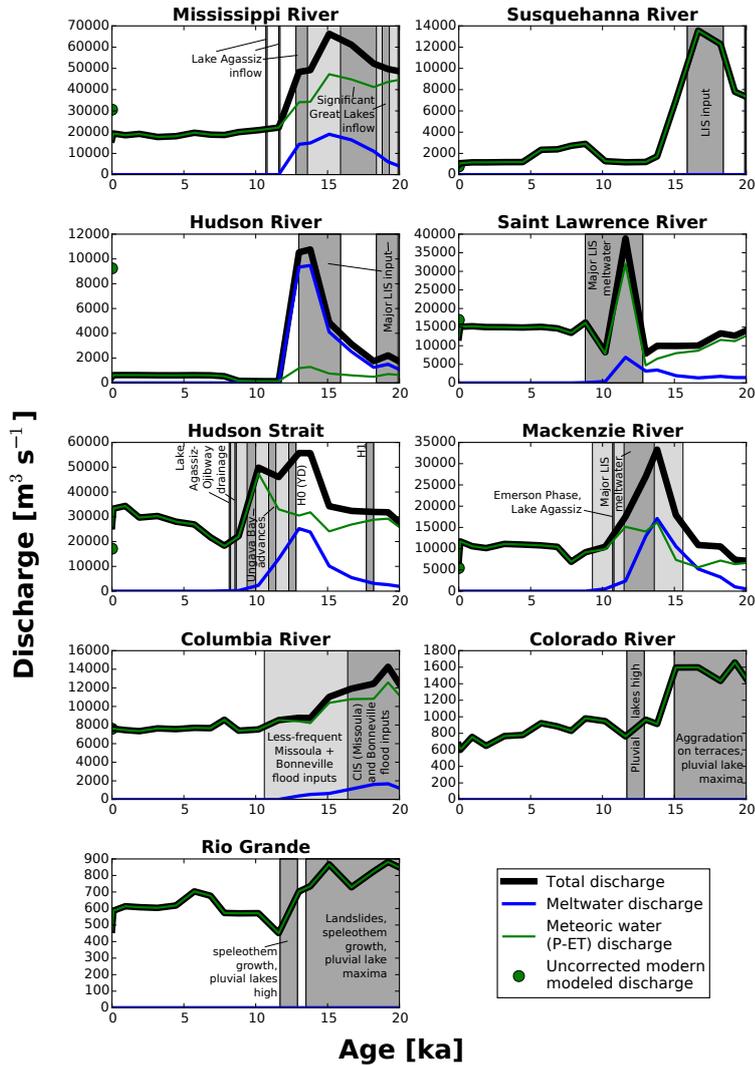
Figure 10. Computed discharge from ICE-3G/VM1 (Tushingham and Peltier, 1991), with gray shading at times of enhanced discharge based on the geologic record. Dark gray indicates a specific time of enhanced discharge, while light gray indicates inferred higher discharge from ice-sheet and landscape geometry or other factors, or, for the Columbia River, a time of enhanced discharge that is likely less-enhanced than earlier in the record. These are annotated here with the following abbreviations: LIS, Laurentide Ice Sheet; H0 (YD) and H1, Heinrich Events 0 (Younger Dryas) and 1; CIS, Cordilleran Ice Sheet.

Earth **Surface**
Dynamics
Discussions
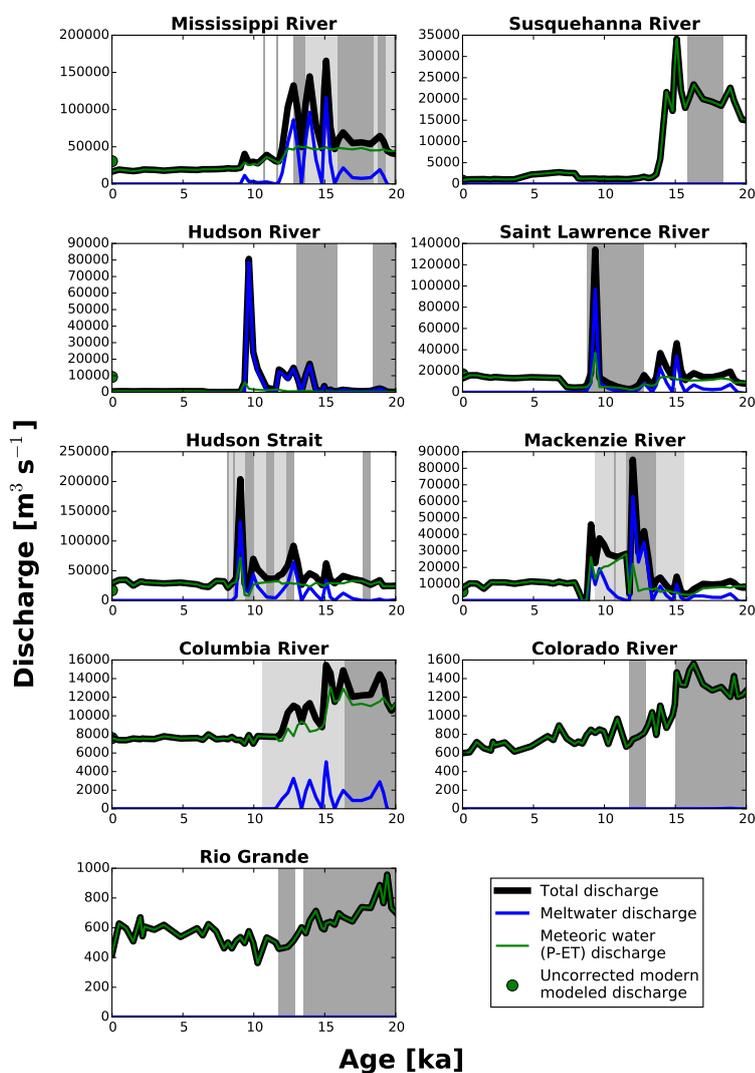
Figure 11. Computed discharge based on the ANU ice-sheet–solid-Earth model pair (Lambeck et al., 2002), compared to the geologic record of enhanced past discharge (gray shading: dark, specific; light, inferred and/or less discharge). Notes on the geologic record can be found in Fig. 10.

Earth **Surface**
Dynamics
Discussions
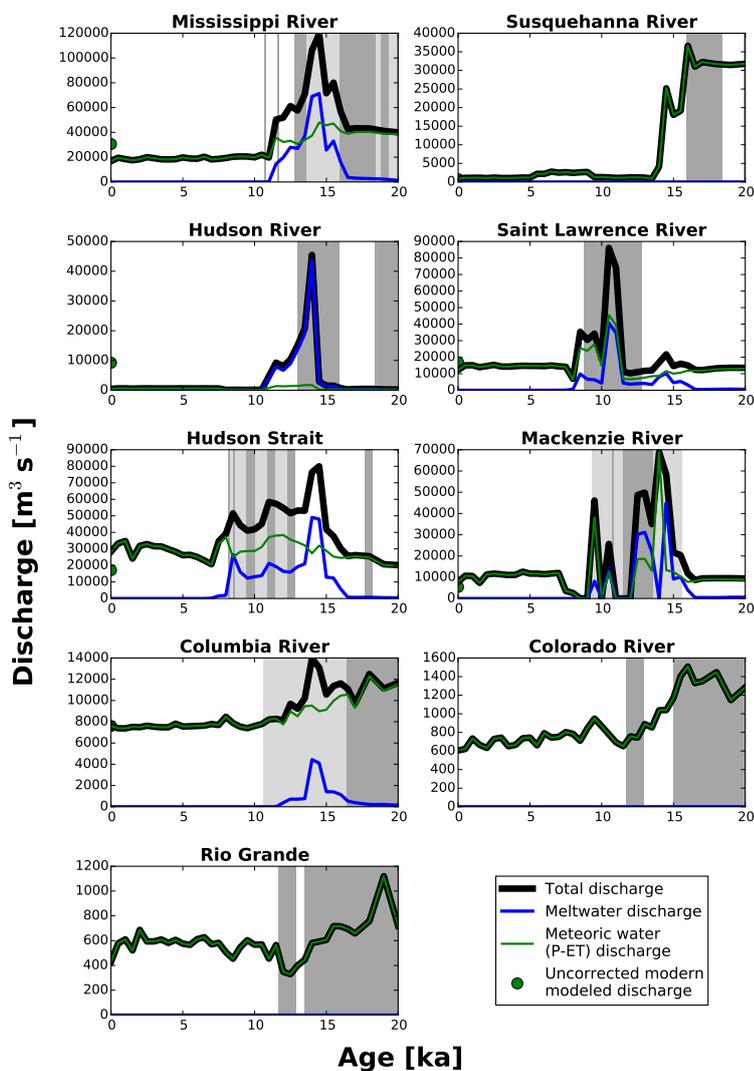
Figure 12. Computed discharge based on ICE-5G/VM2 (Peltier, 2004), compared to the geologic record of enhanced past discharge (gray shading: dark, direct record; light, inferred and/or less discharge). Notes on the geologic record can be found in Fig. 10.
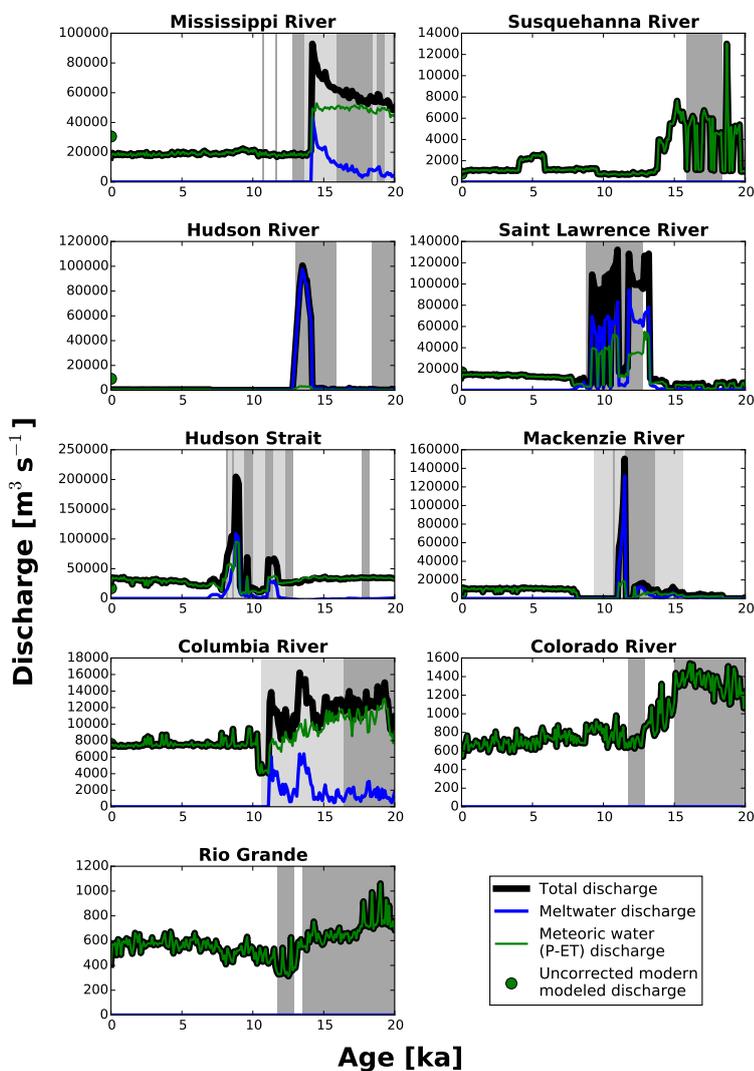
Figure 13. Computed discharge based on the G12/VM2 coupled ice-sheet–solid-Earth model (Gregoire et al., 2012; Peltier, 2004), compared to the geologic record of enhanced past discharge (gray shading: dark, direct record; light, inferred and/or less discharge). Notes on the geologic record can be found in Fig. 10.
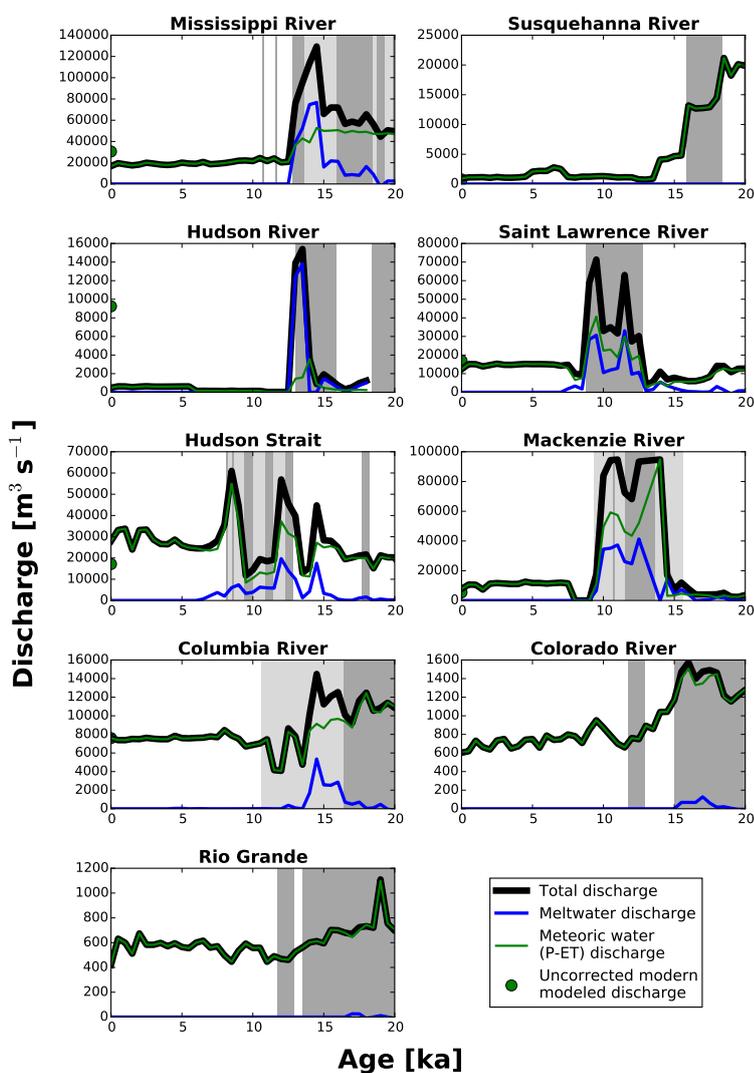
Figure 14. Computed discharge based on the ICE-6G/VM5a coupled ice-sheet–solid-Earth model (Argus et al., 2014; Peltier et al., 2015), compared to the geologic record of enhanced past discharge (gray shading: dark, direct record; light, inferred and/or less discharge). Notes on the geologic record can be found in Fig. 10.
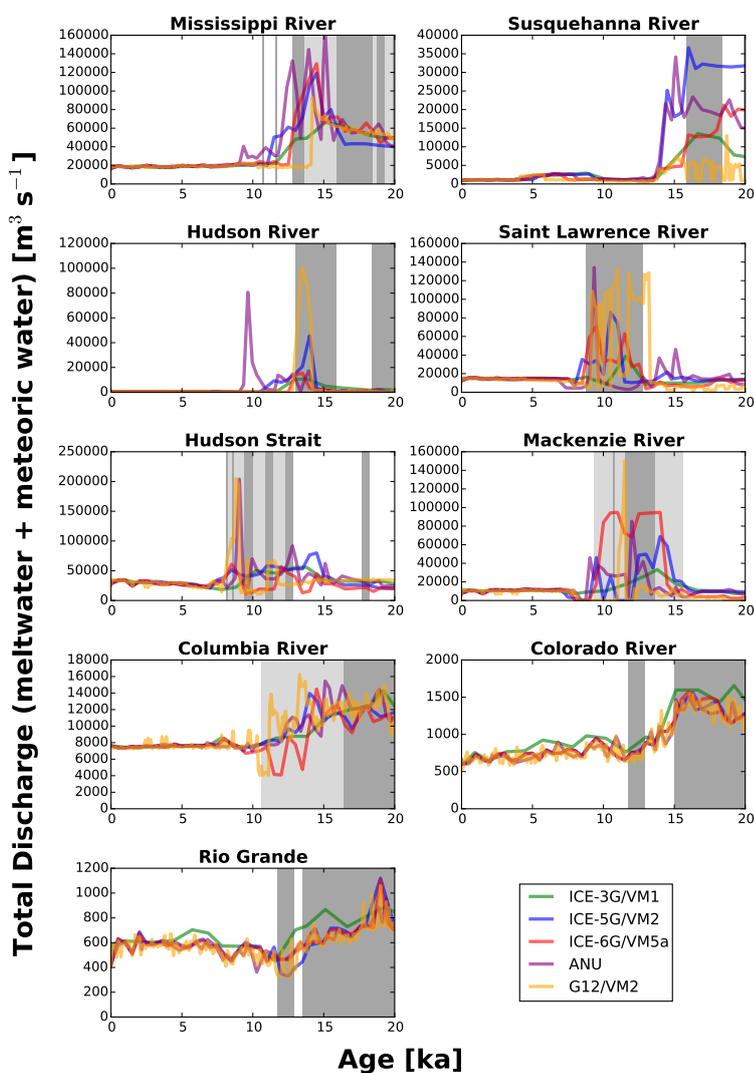
Figure 15. Total discharge from each river basin, represented on a single set of axes for comparison of timing and absolute magnitudes of meltwater discharge among the models, with the geologic record of enhanced past discharge (gray shading: dark, direct record; light, inferred and/or less discharge).

end of the Erie Interstade, at 18.4 ka (Licciardi et al., 1999; Reimer et al., 2013; Wickert, 2014), the Port Bruce Stade advance rerouted all Great Lakes flow to the Mississippi River and produced the Valley Heads Glaciation in New York, sending flow back from the Hudson to the Susquehanna and Mississippi from 18.4–15.9 ka. As the ice again retreated during the 15.9–15.6 ka Mackinaw Interstade, the Hudson took all of the eastern outflow from the Great Lakes, reducing Mississippi discharge and removing ice-sheet inputs from the Susquehanna for the final time. Ice advanced again starting at 15.6 ka towards its Port Huron Stade maximum, returning flow from the Lake Ontario basin to the Hudson River and all other Great Lakes to the Mississippi. After 15.2 ka, the Great Lakes (except for Lake Superior) gradually shifted their flow away from the Mississippi and towards the Hudson, though the Mississippi was augmented by increasing melt via the Des Moines Lobe, James Lobe, and Lake Agassiz (Patterson, 1997, 1998; Licciardi et al., 1999; Sionneau et al., 2010).

Meltwater routing down the Mississippi lasted until ∼12.9 ka (Williams et al., 2012; Wickert et al., 2013), when its last major ice-sheet contributor, the Lake Agassiz drainage basin, was rerouted either east to the newly-ice-free Saint Lawrence (Broecker et al., 1989; Carlson et al., 2007; Carlson and Clark, 2012) or to the Mackenzie River (Murton et al., 2010; Breckenridge, 2015). Regardless of the routing of Lake Agassiz meltwater, a significant amount of meltwater was routed to the Gulf of Saint Lawrence starting at ∼13.2 ka (Carlson et al., 2007; Rayburn et al., 2011). The Saint Lawrence continued to receive significant water inputs via lakes Agassiz and Ojibway until sometime between ∼8.6 ka, the potential subglacial flood from the combined Lake Agassiz-Ojibway into Hudson Bay (Breckenridge et al., 2012), and 8.2 ka, when the ice saddle in Hudson Bay collapsed, causing the 8.2 ka event flood (Barber et al., 1999; Gregoire et al., 2012; Breckenridge et al., 2012; Stroup et al., 2013). While this was the last meltwater input to the Saint Lawrence River, meltwater from the Québec–Labrador dome flowed down the Manicouagan River and into the Gulf of Saint Lawrence until ∼7.8 ka (Occhietti et al., 2004).

The record of pre-Agassiz–Ojibway flood water discharge from Hudson Bay and Hudson Strait, which was an ice-covered marine-terminating margin, comes primarily from records of ice-rafted debris in marine sediment cores. The largest of the post-LGM ice-rafted debris events was Heinrich Event 1, 18.2–17.7 ka (Rashid et al., 2003). Heinrich Event 0, corresponding to the Younger Dryas, was 12.8–12.3 ka (Clark et al., 2001). Later ice-rafting events are related to ice advances in Ungava Bay; these comprise the 11.4–10.9 ka Gold Cove advance (Kaufman and Miller, 1993) and the 10.0–9.4 ka Noble Inlet advance (Metz et al., 2008). Following the ∼8.6 ka possible subglacial drainage of Lake Agassiz–Ojibway, identified by a low-water period in the varve record (Breckenridge et al., 2012), and the 8.2 ka catastrophic drainage (Barber et al., 1999), Hudson Bay was fed by a much lower meltwater input from the ablating remnant Laurentide ice-caps (cf. Dyke et al., 2003; Dyke, 2004), and shrank as isostatic rebound at a time-averaged rate of 1.3 cm yr^{-1} (Lavoie et al., 2012) caused its shoreline to retreat.

The main period of post-LGM high discharge down the Mackenzie River started ∼15.6 ka with the

545   retreat of the Mackenzie Lobe of the Laurentide Ice Sheet and associated meltwater production (Duk-Rodkin et al., 1994; Lemmen et al., 1994). Melt accelerated ∼13.6 ka, when glacial Lake McConnell formed, and between ∼13.6 and ∼13.3 ka catastrophically flooded towards the Mackenzie River. Additional Lake McConnell outburst floods occurred at ∼13.3 (possible but uncertain) and at ∼13.1 ka. At 13.1 ka, ice retreat rerouted Glacial Lake Peace, which formerly drained into the Missouri

550   (and hence, the Mississippi) river, towards the Mackenzie, significantly increasing its drainage area. Between 13.0 and 11.5 ka, large amounts of meltwater continued to be routed down the Mackenzie River. This date range includes the likely timing of the incision of the Mackenzie River ramparts (Mackay and Mathews, 1973; Lemmen et al., 1994; Wickert, 2014), deposition of flood-transported boulders on the Mackenzie River delta (Murton et al., 2010), and a major ∼11.6 ka negative $\delta^{18}O$

555   excursion in the Beaufort Sea (Andrews and Dunhill, 2004). After 11.5 ka, the Laurentide Ice Sheet continued to retreat, feeding meltwater into the Mackenzie River system that included a 10.8–10.7 ka flood from Lake Agassiz during its Emerson phase (Fisher and Lowell, 2012). The retreating Laurentide Ice Sheet left the Mackenzie basin by ∼9.3 ka (Lemmen et al., 1994).

The Columbia River has an offshore record of rapid turbidite deposition that stretches 36.1–10.6

560   ka (Zuffa et al., 2000). Within this time, large floods associated with glacial Lake Missoula occurred 22.9–16.5 ka (Bretz, 1923, 1969; Waitt, 1980; Atwater, 1984; Benito and O'Connor, 2003), and Lake Bonneville routed a portion of flow from the Great Basin to the Columbia River 18.2–16.4 ka (Gilbert, 1890; Godsey et al., 2005, 2011; McGee et al., 2012). The terrestrial record contains evidence for later, smaller outflows from glacial Lake Missoula 15.1–12.6 ka (Hanson et al., 2012),

565   and intermittent overflow inputs from Lake Bonneville 16.4–14.8 ka (synthesis of Godsey et al., 2011; McGee et al., 2012).

The Colorado River and the Rio Grande, while influenced by mountain glacier retreat, experienced different discharges largely due to the wetter climate in their drainage basins during the Last Glacial Maximum and Younger Dryas. These cool, wet periods are marked by high lake levels (e.g., Currey

570   et al., 1990; Matsubara and Howard, 2009; McGee et al., 2012), mountain glacier advances prior to the onset of the Bølling-Allerød (e.g., Owen et al., 2003; Guido et al., 2007; Orme, 2008), increased landsliding in the Rio Grande basin between ∼21.2 and ∼14.5 ka (Reneau and Dethier, 1996), and speleothem growth (Polyak et al., 2004). This pattern of climate change closely mirrors that seen in Greenland (Benson et al., 1997; Svensson et al., 2008; Asmerom et al., 2010; Wagner et al., 2010).

575   **5.1.2   Comparison of data and models for river discharge**

In order to determine how well, broadly, these different models were able to reproduce discharge, I subdivided the computed discharges into events during known high-flow periods (light and dark gray regions on Figs.10–15 and those from the low-flow remainder of the record. I first compared the mean discharges during known high- and low-flow periods (Fig. 16A). For the five ice-sheet models

580   and nine river systems, only once did the known low-flow time produce a higher computed discharge
(the Hudson River for the ANU model). The ice-physics-based G12 performed the best in generat-
ing discharges during high-flow periods that were much higher than those during low-flow periods.
I then generated histograms for the high-flow and low-flow segments of the model results, and per-
formed Kolmogorov–Smirnov tests between the pairs of distributions for each ice model and river

585   system to test how different they are from one another (Fig. 16B). Here, the new GIA-based ICE-6G
performed the best and G12 performed the worst. While visual inspection of Figure 13 shows that
G12 performs quite well in representing general patterns of deglacial water discharge, including the
pulses of meltwater output from Hudson Strait associated that would produce the diagnostic iceberg
pulses of Heinrich events (e.g., Heinrich, 1988; Andrews and MacLean, 2003; Hemming, 2004),

590   its short (but intense) pulse down the Mackenzie River and lack of early meltwater down the Hud-
son River reduced the average, and the averaging across the longer meltwater-production period for
Hudson Strait reduced the goodness-of-fit. G12 is also affected by a too-early switch of meltwater
outflow away from the Mississippi River because its climate forcing and dynamical ice response
created a Québec–Labrador dome that retreats too soon.

595   Across all model runs, Hudson Bay was the consistent site of the worst data–model comparisons.
It is possible that this is due to data-collection issues (e.g., few organics) and data sparsity (few
settlements and fewer GPS monuments) in this formerly fully ice-covered region, leading to a lack
of good regional constraints on ice-sheet thickness near the center of the Laurentide Ice Sheet. Or,
on the other hand, this could be because the models do not accurately represent the dynamics of the

600   marine-terminating Hudson Strait ice catchment (e.g., MacAyeal, 1993).

5.1.3   Comparison of data and models for drainage basin extents

All of the simulated ice sheets follow the broad strokes of the expected pattern of drainage. This
is as would be expected: any effort to put a realistically-shaped ice sheet onto North America will
cause more flow to be routed towards the Mississippi River and less to the Saint Lawrence River.

605   This section covers examples of where the ice-sheet models did not match the data-driven drainage
basin extents, and concludes with suggestions for how to improve such fits.

At the Last Glacial Maximum, ICE-5G and G12 have the most severe misfits with data. ICE-5G
sends a large fraction of Mississippi-River-bound drainage to the Hudson River, an artifact fixed in
ICE-6G with its more realistic ice-dome structure. G12 at the Last Glacial Maximum has Macken-

610   zie River drainage routed towards the Yukon River, though time-steps shortly before and after the
LGM have the proper drainage routing. This underscores the importance of drainage routing as a
discriminating factor in ice-sheet-model quality, as it is able to detect thresholds in ice-sheet thick-
ness that are required to maintain a realistic ice geometry. ANU and G12 produce the most realistic
flow partitioning between the Susquehanna and Hudson Rivers.
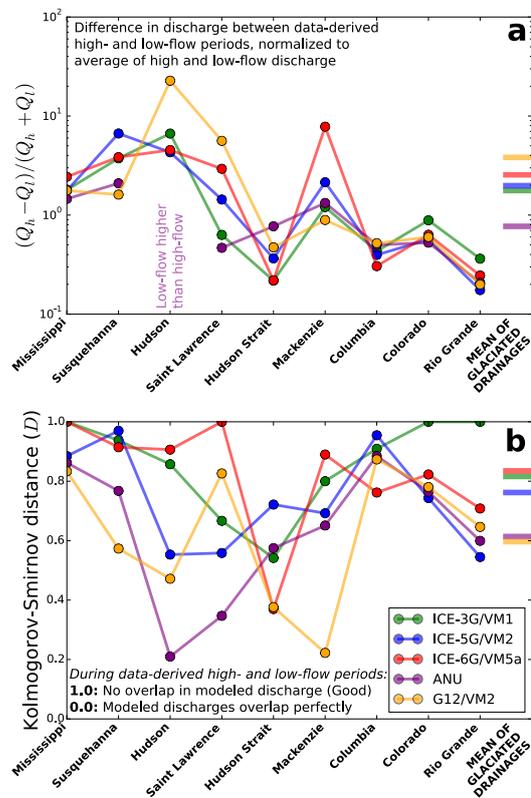
Figure 16. The computed discharge time-series is segmented into values corresponding with times of known high and low discharge. **a.** Normalized difference between known high and low discharge times. The greatest mean normalized difference is seen in G12, the ice-physics based model of Gregoire et al. (2012), and the least in the GIA-based model of Lambeck et al. (2002). **b.** The Kolmogorov–Smirnov test measures the distance between one-dimensional distributions; here I use it to compute the a metric of difference between the computed discharge histograms for each river system during the generalized data-derived times of high and low discharge (both light and dark gray in Figs. 10–15). A high distance value indicates a strong separation between the range of discharges during geologically-constrained high- and low-flow periods, and hence a good match between the data and model. Here, the new GIA-based ICE-6G model performs the best, with a strong match to all but the Hudson Bay record, and the ice-physics-based G12 performs the worst, due in part to the too-early demise of its Québec–Labrador dome.

615   During Bølling-Allerød time, only ICE-6G and G12 properly show that ice retreated beyond the
bounds of the Susquehanna River basin. All models simulate the Mississippi and Mackenzie catch-
ments generally well, and close to what available data (e.g., Margold et al., 2014) would indicate.

During the early part of the Younger Dryas, the Mackenzie and Saint Lawrence Rivers both expe-
rienced periods of high discharge (de Vernal et al., 1996; Carlson et al., 2007; Murton et al., 2010). It
620   is unclear whether their basins tapped into the center of the continent: debate continues as to whether
Lake Agassiz flowed towards the Mackenzie River in the northwest (e.g., Murton et al., 2010; Breck-
enridge, 2015), towards the Saint Lawrence River in the east (e.g., Carlson and Clark, 2012), or, as
one group has proposed, became a closed basin at this time due to regional drying (Lowell et al.,
2013). Currently, the most favorable hypothesis seems to be a northwesterly route, which is consis-
625   tent with the newly-remapped strandlines (Breckenridge, 2015). The drying hypothesis seems the
least likely, as the model simulate it (Lowell et al., 2013) creates a closed basin when at least two
parameters seem unreasonable. These are (1) evaporative loss that is generally >1.5 times today's
observations, in spite of cooler temperatures and a longer lake-ice season, and (2) a temperature
lapse rate that is 7.3 °C km^{-1}, outside of the error bars of the 5.1±1.2 °C km^{-1} observed on mod-
630   ern ice sheets and ice caps Anderson et al. (2014), and resulting in a smaller melt-producing area of
the Laurentide Ice Sheet. Regardless of where Lake Agassiz flowed, or whether it became a closed
basin (the flow-routing presented here does not allow closed basins to exist: see Section 2.3.2), iso-
topic data from the Gulf of Mexico show unequivocally that meltwater discharge to the Mississippi
ended ∼12.9 ka (Wickert et al., 2013). This means that the ICE-5G and ANU reconstructions miss
635   the timing of the most major drainage rearrangement in the North American deglaciation. The G12
reconstruction has such intense isostatic adjustment when coupled with the VM2 solid Earth model
that there is marine inundation of the entire set of Great Lakes Basins, and the Upper Missouri River
in G12 and ICE-6G flows towards the north. In G12, this is due in part to the too-early retreat of the
southeastern Laurentide margin. Overall, ICE-3G and ICE-6G perform the best, with the latter send-
640   ing Lake Agassiz meltwater to the Mackenzie River and Beaufort Sea and water from the Laurentide
Great Lakes to the Gulf of Saint Lawrence, a scenario that is consistent with current geological ev-
idence (e.g., de Vernal et al., 1996; Richard et al., 2005; Carlson et al., 2007; Murton et al., 2010;
Rayburn et al., 2011; Breckenridge, 2015).

The early Holocene in northern North America was characterized by retreat of the Laurentide Ice
645   Sheet that led to expansion of proglacial lakes, setting the stage for the short-lived and rapid 8.2
ka cooling event (Breckenridge et al., 2012). G12 produced a saddle collapse that led to this flood
(Gregoire et al., 2012), though with a somewhat different spatial pattern than what has been mapped
(Dyke et al., 2003; Dyke, 2004). None of the models perform particularly well here. ICE-3G has
altogether too much ice retreat. ICE-5G, ICE-6G, and ANU have a drainage divide that splits the
650   large east–west Saint Lawrence drainage basin, which is constrained by the dual facts that Lake
Agassiz drained the Canadian Rockies and, at this time, flowed via the Ottawa River to the Saint

Lawrence (Teller and Leverington, 2004; Breckenridge et al., 2012; Stroup et al., 2013). G12 has such a continuous drainage basin, but it flows out a gap along the southwest corner of the retreating ice-sheet, and from there, flows to the Arctic instead of to the Saint Lawrence. It is notable that ICE-5G, ICE-6G, and G12 have a tiny Mackenzie River basin due to glacial isostatic adjustment, and evaluating the plausibility of this could be a goal for future field work.

5.2 Future directions: coupling with hydrologic, climate, isotopic, archaeological, and sediment transport models and observations

The work presented here is a necessary starting point for future studies on the interactions between deglacial surface-water hydrology and other components of the integrated Earth system. Combining these meltwater routing patterns with proglacial lakes and changing land cover will allow equations designed to predict sediment yield from large catchments to be employed for a continental-scale paleo-sediment-discharge reconstruction (following Overeem et al., 2005; Kettner and Syvitski, 2008; Pelletier, 2012; Cohen et al., 2013), with modern control provided by present-day sediment yields (Table 1). These sediment discharges can be compared with records of deposition (e.g., Andrews and Dunhill, 2004; Breckenridge, 2007; Williams et al., 2010) and records of geomorphic change (e.g., Reusser et al., 2006; Knox, 2007; Anderson, 2015). The need to properly compute past lake and land cover motivates continued work with climate- and water-balance models (e.g., Collins et al., 2006; Matsubara and Howard, 2009; Liu et al., 2009; He, 2011; Blois et al., 2013). These, together with paleogeographic reconstructions such as those presented here, can be used to reconstruct areas of archaeological interest, either as changes in shoreline positions and topography (Clark et al., 2014) or as a wholesale landscape reconstruction that incorporates site-potential modeling (Monteleone et al., 2013; Monteleone, 2013; Dixon and Monteleone, 2014). On a global scale, several current flow-routing algorithms could be made global for better integration with ice-sheet, climate, and GIA models (Metz et al., 2011; Qin and Zhan, 2012; Braun and Bezada, 2013; Huang and Lee, 2013; Schwanghart and Scherler, 2014), including the possibility to include high-resolution flow routing as part of a transient coupled model run instead of an *a posteriori* analysis, as is presented here. Finally, high-resolution drainage routing schemes can connect models of past climate, ice sheets, and drainage routing, to oxygen isotopes in sediment cores (Wickert et al., 2013), and the increasingly-complete collection of such records from the North American continental margin (Andrews et al., 1994; de Vernal et al., 1996; Brown, 2011; Williams et al., 2012; Gibb et al., 2014; Taylor et al., 2014) is opening new possibilities in isotopic studies of whole-ice-sheet mass balance.

6 Conclusions

The goal of this work is to move towards a self-consistent paleogeographic framework within which models and geologic records may be quantitatively compared to build new insights into past glacial

systems and climate–ice-sheet interactions. Most ice-sheet reconstructions are built to fit glacial iso-static adjustment measurements and moraine positions, and/or by using ice-physics-based models. These are not calibrated to drainage basins and meltwater pathways, even though these leave behind geomorphic and stratigraphic markers that can be used to discriminate between hypothesized ice-

690 thickness distributions and deglaciation histories. The dynamic deglacial drainage basins of North America are significant in their own right, and the new paleohydrographs presented here can help us to better understand the ice-age legacy imprinted on the major rivers of North America. When integrated more broadly into studies of North American deglaciation, these time-varying deglacial drainage basins and paleohydrographs are poised to improve reconstructions of past climate and

695 ice-sheet geometry.

References

705   Adler, R. F., Huffman, G. J., Chang, A., Ferraro, R., Xie, P.-P., Janowiak, J., Rudolf, B., Schneider, U., Curtis, S., Bolvin, D., Gruber, A., Susskind, J., Arkin, P., and Nelkin, E.: The Version-2 Global Precipitation Climatology Project (GPCP) Monthly Precipitation Analysis (1979–Present), Journal of Hydrometeorology, 4, 1147–1167, doi:10.1175/1525-7541(2003)004<1147:TVGPCP>2.0.CO;2, 2003.

Alden, W. C.: Physiography and glacial geology of western Montana and adjacent areas, vol. 231 of *Profes-*
710   *sional Paper 174*, United States Geological Survey, 1932.

Amante, C. and Eakins, B. W.: ETOPO1 1 Arc-Minute Global Relief Model: Procedures, Data Sources and Analysis, NOAA Technical Memorandum NESDIS NGDC-24, 2009.

Anderson, J.: History of the Missouri River Valley from the Late Pleistocene to Present : Climatic vs . Tectonic Forcing on Valley Architecture, M.s. thesis, Texas Christian University, 2015.

715   Anderson, L. S., Roe, G. H., and Anderson, R. S.: The effects of interannual climate variability on the moraine record, Geology, 42, 55–58, doi:10.1130/G34791.1, 2014.

Anderson, R. C.: Reconstruction of preglacial drainage and its diversion by earliest glacial forebulge in the upper Mississippi Valley region, Geology, 16, 254, 1988.

Andersson, A., Fennig, K., Klepp, C., Bakan, S., Graß l, H., and Schulz, J.: The Hamburg Ocean Atmo-
720   sphere Parameters and Fluxes from Satellite Data – HOAPS-3, Earth System Science Data, 2, 215–234, doi:10.5194/essd-2-215-2010, 2010.

Andersson, A., Klepp, C., Fennig, K., Bakan, S., Grassl, H., and Schulz, J.: Evaluation of HOAPS-3 Ocean Surface Freshwater Flux Components, Journal of Applied Meteorology and Climatology, 50, 379–398, doi:10.1175/2010JAMC2341.1, 2011.

725   Andrews, J. T. and Dunhill, G.: Early to mid-Holocene Atlantic water influx and deglacial meltwater events, Beaufort Sea slope, Arctic Ocean, Quaternary Research, 61, 14–21, doi:10.1016/j.yqres.2003.08.003, 2004.

Andrews, J. T. and MacLean, B.: Hudson Strait ice streams: a review of stratigraphy, chronology and links with North Atlantic Heinrich events, Boreas, 32, 4–17, doi:10.1080/03009480310001010, 2003.

Andrews, J. T. and Tedesco, K.: Detrital carbonate-rich sediments, northwestern Labrador Sea: Implications
730   for ice-sheet dynamics and iceberg rafting (Heinrich) events in the North Atlantic, Geology, 20, 1087–1090, doi:10.1130/0091-7613(1992)020<1087:DCRSNL>2.3.CO;2, 1992.

Andrews, J. T., Erlenkeuser, H., Tedesco, K., Aksu, A. E., and Jull, A.: Late Quaternary (Stage 2 and 3) Meltwater and Heinrich Events, Northwest Labrador Sea, Quaternary Research, 41, 26–34, doi:10.1006/qres.1994.1003, 1994.

735   Andrews, J. T., Keigwin, L., Hall, F., and Jennings, A. E.: Abrupt deglaciation events and Holocene palaeoceanography from high-resolution cores, Cartwright Saddle, Labrador Shelf, Canada, Journal of Quaternary Science, 14, 383–397, doi:10.1002/(SICI)1099-1417(199908)14:5<383::AID-JQS464>3.0.CO;2-J, 1999.

Antevs, E.: The recession of the last ice sheet in New England, Research Series, American Geographical Society, 1922.

740   Argus, D. F. and Peltier, W. R.: Constraining models of postglacial rebound using space geodesy: a detailed assessment of model ICE-5G (VM2) and its relatives, Geophysical Journal International, 181, 697–723, doi:10.1111/j.1365-246X.2010.04562.x, 2010.

Earth **Surface**
Dynamics
Discussions

Argus, D. F., Peltier, W. R., Drummond, R., and Moore, a. W.: The Antarctica component of postglacial rebound model ICE-6G_C (VM5a) based on GPS positioning, exposure age dating of ice thicknesses, and relative

745   sea level histories, Geophysical Journal International, 198, 537–563, doi:10.1093/gji/ggu140, 2014.

Asmerom, Y., Polyak, V. J., and Burns, S. J.: Variable winter moisture in the southwestern United States linked to rapid glacial climate shifts, Nature Geoscience, 3, 114–117, doi:10.1038/ngeo754, 2010.

Atwater, B. F.: Periodic floods from glacial Lake Missoula into the Sanpoil arm of glacial Lake Columbia, north-eastern Washington, Geology, 12, 464–467, doi:10.1130/0091-7613(1984)12<464:PFFGLM>2.0.CO;2,

750   1984.

Austermann, J., Mitrovica, J. X., Latychev, K., and Milne, G. A.: Barbados-based estimate of ice volume at Last Glacial Maximum affected by subducted plate, Nature Geoscience, 6, 553–557, doi:10.1038/ngeo1859, 2013.

Barber, D. C., Jennings, A. E., Andrews, J. T., Kerwin, M. W., and Morehead, M. D.: Forcing of the cold event

755   of 8,200 years ago by catastrophic drainage of Laurentide lakes, Nature, 400, 13–15, doi:10.1038/22504, 1999.

Benito, G. and O'Connor, J. E.: Number and size of last-glacial Missoula floods in the Columbia River valley between the Pasco Basin, Washington, and Portland, Oregon, Geological Society of America Bulletin, 115, 624–638, doi:10.1130/0016-7606(2003)115<0624:NASOLM>2.0.CO;2, 2003.

760 Benson, L., Burdett, J., Lund, S., Kashgarian, M., and Mensing, S.: Nearly synchronous climate change in the Northern Hemisphere during the last glacial termination, Nature, 388, 263–265, 1997.

Bentley, S.: Fluvial Sediment Delivery to Hudson Bay in a Changing Climate: Projections and Hypotheses, in: ArcticNet Annual Scientific Meeting, Victoria, British Columbia, Canada, 2006.

Blois, J. L., Williams, J. W., Fitzpatrick, M. C., Ferrier, S., Veloz, S. D., He, F., Liu, Z., Manion, G., and

765   Otto-Bliesner, B.: Modeling the climatic drivers of spatial patterns in vegetation composition since the Last Glacial Maximum, Ecography, 36, 460–473, doi:10.1111/j.1600-0587.2012.07852.x, 2013.

Bluemle, J. P.: Pleistocene Drainage Development in North Dakota, Geological Society of America Bulletin, 83, 2189, doi:10.1130/0016-7606(1972)83[2189:PDDIND]2.0.CO;2, 1972.

Blumentritt, D. J., Wright, H. E., and Stefanova, V.: Formation and early history of Lakes Pepin and St. Croix

770   of the upper Mississippi River, Journal of Paleolimnology, 41, 545–562, 2009.

Braun, C. and Bezada, M.: The History and Disappearance of Glaciers in Venezuela, Journal of Latin American Geography, 12, 85–124, doi:10.1353/lag.2013.0016, 2013.

Breckenridge, A.: The Lake Superior varve stratigraphy and implications for eastern Lake Agassiz outflow from 10,700 to 8900 cal ybp (9.5–8.0 ^{14}C ka), Palaeogeography, Palaeoclimatology, Palaeoecology, 246,

775   45–61, doi:10.1016/j.palaeo.2006.10.026, 2007.

Breckenridge, A.: The Tintah-Campbell gap and implications for glacial Lake Agassiz drainage during the Younger Dryas cold interval, Quaternary Science Reviews, 117, 124–134, doi:10.1016/j.quascirev.2015.04.009, 2015.

Breckenridge, A., Lowell, T. V., Stroup, J. S., and Evans, G.: A review and analysis of varve thickness

780   records from glacial Lake Ojibway (Ontario and Quebec, Canada), Quaternary International, 260, 43–54, doi:10.1016/j.quaint.2011.09.031, 2012.

Bretz, J.: The channeled scablands of the Columbia Plateau, The Journal of Geology, 31, 617–649, 1923.

Bretz, J. H.: The Lake Missoula floods and the channeled scabland, The Journal of Geology, 77, 505–543, 1969.

British Oceanographic Data Centre (BaODC) and General Bathymetric Chart of the Oceans (GEBCO): The
785   GEBCO_08 Grid, version 20100927, 2010.

Broecker, W. S., Kennett, J. P., Flower, B. P., Teller, J. T., Trumbore, S., Bonani, G., and Wolfli, W.: Routing
     of meltwater from the Laurentide Ice Sheet during the Younger Dryas cold episode, Nature, 341, 318–321,
     doi:10.1038/341318a0, 1989.

Brown, E. A.: Initial Ablation of the Laurentide Ice Sheet Based on Gulf of Mexico Sediments, M.s. thesis,
790   University of South Florida, 2011.

Carlson, A. E. and Clark, P. U.: Ice sheet sources of sea level rise and freshwater discharge during the last
     deglaciation, Reviews of Geophysics, 50, RG4007, doi:10.1029/2011RG000371, 2012.

Carlson, A. E., Clark, P. U., Haley, B. a., Klinkhammer, G. P., Simmons, K., Brook, E. J., and Meissner,
     K. J.: Geochemical proxies of North American freshwater routing during the Younger Dryas cold event.,
795   Proceedings of the National Academy of Sciences of the United States of America, 104, 6556–6561,
     doi:10.1073/pnas.0611313104, 2007.

Carriquiry, J. D. and Sánchez, A.: Sedimentation in the Colorado River delta and Upper Gulf of California after
     nearly a century of discharge loss, Marine Geology, 158, 125–145, doi:10.1016/S0025-3227(98)00189-3,
     1999.

800 Carson, M. A., Jasper, J. N., and Conly, F. M.: Magnitude and sources of sediment input to the Mackenzie Delta,
     Northwest Territories, 1974–94, Arctic, 51, 116–124, 1998.

Chen, M., Xie, P., Janowiak, J. E., and Arkin, P. A.: Global Land Precipitation: A 50-yr Monthly
     Analysis Based on Gauge Observations, Journal of Hydrometeorology, 3, 249–266, doi:10.1175/1525-
     7541(2002)003<0249:GLPAYM>2.0.CO;2, 2002.

805 Clague, J. J. and James, T. S.: History and isostatic effects of the last ice sheet in southern British Columbia,
     Quaternary Science Reviews, 21, 71–87, doi:10.1016/S0277-3791(01)00070-1, 2002.

Clark, J., Mitrovica, J. X., and Alder, J.: Coastal paleogeography of the California–Oregon–Washington and
     Bering Sea continental shelves during the latest Pleistocene and Holocene: implications for the archaeologi-
     cal record, Journal of Archaeological Science, 52, 12–23, doi:10.1016/j.jas.2014.07.030, 2014.

810 Clark, P. U., Marshall, S. J., Clarke, G. K. C., Hostetler, S. W., Licciardi, J. M., and Teller, J. T.: Freshwa-
     ter forcing of abrupt climate change during the last glaciation., Science (New York, N.Y.), 293, 283–7,
     doi:10.1126/science.1062517, 2001.

Clark, P. U., Dyke, A. S., Shakun, J. D., Carlson, A. E., Clark, J., Wohlfarth, B., Mitrovica, J. X., Hostetler,
     S. W., McCabe, A. M., Clark, P. U., Dyke, A. S., Shakun, J. D., Carlson, A. E., Clark, J., Wohlfarth, B.,
815   Mitrovica, J. X., Hostetler, S. W., and McCabe, A. M.: The Last Glacial Maximum., Science, 325, 710–714,
     doi:10.1126/science.1172873, 2009.

Cohen, M. J., Henges-Jeck, C., and Castillo-Moreno, G.: A preliminary water balance for the Colorado River
     delta, 1992–1998, Journal of Arid Environments, 49, 35–48, doi:10.1006/jare.2001.0834, 2001.

Cohen, S., Kettner, A. J., Syvitski, J. P. M., and Fekete, B. M.: WBMsed, a distributed global-scale river-
820   ine sediment flux model: Model description and validation, Computers and Geosciences, 53, 80–93,
     doi:10.1016/j.cageo.2011.08.011, 2013.

Collins, W. D., Bitz, C. M., Blackmon, M. L., Bonan, G. B., Bretherton, C. S., Carton, J. A., Chang, P., Doney, S. C., Hack, J. J., Henderson, T. B., Kiehl, J. T., Large, W. G., McKenna, D. S., Santer, B. D., and Smith, R. D.: The Community Climate System Model Version 3 (CCSM3), Journal of Climate, 19, 2122–2143,
825   doi:10.1175/JCLI3761.1, 2006.

Condron, A. and Winsor, P.: Meltwater routing and the Younger Dryas., Proceedings of the National Academy of Sciences of the United States of America, 109, 19 928–19 933, doi:10.1073/pnas.1207381109, 2012.

Cuffey, K. M. and Paterson, W. S. B.: The physics of glaciers, Academic Press, Oxford, UK, 4th edn., 2010.

Currey, D. R., V, E. S. P. B., and City, S. L.: Quaternary palaeolakes in the evolution of semidesert basins,
830   with special emphasis on Lake Bonneville and the Great Basin, U.S.A, Palaeogeography, Palaeoclimatology, Palaeoecology, 76, 189–214, doi:10.1016/0031-0182(90)90113-L, 1990.

Curry, B. B.: Evidence at Lomax, Illinois, for Mid-Wisconsin (˜40,000 yr B.P.) Position of the Des Moines Lobe and for Diversion of the Mississippi River by the Lake Michigan Lobe (20,350 yr B.P.), Quaternary Research, 50, 128–138, doi:10.1006/qres.1998.1985, 1998.

835   Curry, B. B., Hajic, E. R., Clark, J. A., Befus, K. M., Carrell, J. E., and Brown, S. E.: The Kankakee Torrent and other large meltwater flooding events during the last deglaciation, Illinois, USA, Quaternary Science Reviews, 90, 22–36, doi:10.1016/j.quascirev.2014.02.006, 2014.

de Vernal, A., Hillaire-Marcel, C., and Bilodeau, G.: Reduced meltwater outflow from the Laurentide ice margin during the Younger Dryas, Nature, 381, 774–777, doi:10.1038/381774a0, 1996.

840   Dean, J. F. and Phillips, B. A. M.: Pre-and-early Agassiz outlets to the western Superior Basin, in: Archean to Anthropocene: Field Guides to the Geology of the Mid-Continent of North America, edited by Miller, J. D., Hudak, G. J., Wittkop, C., and McLaughlin, P. I., Geological Society of America Field Guide, pp. 317–349, Geological Society of America, doi:10.1130/2011.0024(15)., 2011.

Deschamps, P., Durand, N., Bard, E., Hamelin, B., Camoin, G., Thomas, A. L., Henderson, G. M., Okuno, J.,
845   and Yokoyama, Y.: Ice-sheet collapse and sea-level rise at the Bølling warming 14,600 years ago, Nature, 483, 559–564, doi:10.1038/nature10902, 2012.

Dierckx, P.: Curve and surface fitting with splines, Curve and Surface Fitting with Splines, p. 308, doi:10.1093/imamat/1.2.164, 1993.

Dixon, J. E. and Monteleone, K.: Gateway to the Americas: Underwater Archeological Survey in Beringia and
850   the North Pacific, in: Prehistoric Archaeology on the Continental Shelf, chap. 6, pp. 95–114, Springer New York, New York, NY, doi:10.1007/978-1-4614-9635-9_6, 2014.

Dolgopolova, E. N. and Isupova, M. V.: Water and sediment dynamics at Saint Lawrence River mouth, Water Resources, 38, 453–469, doi:10.1134/S009780781104004X, 2011.

Doyon, P.: Seasonal Structure of the Gulf of St. Lawrence Upper-Layer Thermohaline Fields during the Ice-free
855   Months, Ms, McGill University, 1996.

Duk-Rodkin, A., Hughes, O. L., Survey, G., and Calgary, S. N. W.: Tertiary-quaternary drainage of the Pre-glacial Mackenzie basin, Quaternary International, 22-23, 221–241, doi:10.1016/1040-6182(94)90015-9, 1994.

Dutton, A. and Lambeck, K.: Ice Volume and Sea Level During the Last Interglacial, Science, 337, 216–219,
860   doi:10.1126/science.1205749, 2012.

Dyke, A.: An outline of North American deglaciation with emphasis on central and northern Canada, in: Quaternary Glaciations–Extent and Chronology — Part II: North America, edited by Ehlers, J. and Gibbard, P. L., vol. 2 of *Developments in Quaternary Sciences*, pp. 373–424, 2004.

Dyke, A. S. and Prest, V. K.: Late Wisconsinan and Holocene History of the Laurentide Ice Sheet, Géographie physique et Quaternaire, 41, 237, doi:10.7202/032681ar, 1987.

Dyke, A. S., Moore, A., and Robertson, L.: Deglaciation of North America, Open File 1574, Natural Resources Canada, Ottawa, 2003.

Environment Canada: St. Lawrence River: http://www.ec.gc.ca/stl/, 2013.

Fairbanks, R. G.: A 17, 000-year glacio-eustatic sea level record: influence of glacial melting rates on the Younger Dryas event and deep-ocean circulation, Nature, 342, 637–642, 1989.

Fisher, T. G. and Lowell, T. V.: Testing northwest drainage from Lake Agassiz using extant ice margin and strandline data, Quaternary International, 260, 106–114, doi:10.1016/j.quaint.2011.09.018, 2012.

Fisher, T. G. and Souch, C.: Northwest outlet channels of Lake Agassiz, isostatic tilting and a migrating continental drainage divide, Saskatchewan, Canada, Geomorphology, 25, 57–73, doi:10.1016/S0169-555X(98)00028-2, 1998.

Flower, B. P., Hastings, D. W., Hill, H. W., and Quinn, T. M.: Phasing of deglacial warming and Laurentide Ice Sheet meltwater in the Gulf of Mexico, Geology, 32, 597, doi:10.1130/G20604.1, 2004.

Gates, L. D., Hagemann, S., and Golz, C.: Observed historical discharge data from major rivers for climate model validation, Tech. Rep. 307, Max-Planck-Institut für Meterologie, Hamburg, Germany, 2000.

Gibb, O. T., Hillaire-Marcel, C., and de Vernal, A.: Oceanographic regimes in the northwest Labrador Sea since Marine Isotope Stage 3 based on dinocyst and stable isotope proxy records, Quaternary Science Reviews, 92, 269–279, doi:10.1016/j.quascirev.2013.12.010, 2014.

Gilbert, G. K.: Lake Bonneville, U.S. Geological Survey Monograph, US Geological Survey, 1890.

Godsey, H. S., Currey, D. R., and Chan, M. a.: New evidence for an extended occupation of the Provo shoreline and implications for regional climate change, Pleistocene Lake Bonneville, Utah, USA, Quaternary Research, 63, 212–223, 2005.

Godsey, H. S., Oviatt, C. G., Miller, D. M., and Chan, M. a.: Stratigraphy and chronology of offshore to nearshore deposits associated with the Provo shoreline, Pleistocene Lake Bonneville, Utah, Palaeogeography, Palaeoclimatology, Palaeoecology, 310, 442–450, doi:10.1016/j.palaeo.2011.08.005, 2011.

Gowan, E. J.: An assessment of the minimum timing of ice free conditions of the western Laurentide Ice Sheet, Quaternary Science Reviews, 75, 100–113, doi:10.1016/j.quascirev.2013.06.001, 2013.

GRASS Development Team: Geographic Resources Analysis Support System (GRASS GIS) Software, 2012.

Gregoire, L. J., Payne, A. J., and Valdes, P. J.: Deglacial rapid sea level rises caused by ice-sheet saddle collapses, Nature, 487, 219–222, doi:10.1038/nature11257, 2012.

Gross, M. G., Karweit, M., Cronin, W. B., and Schubel, J. R.: Suspended sediment discharge of the Susquehanna River to northern Chesapeake Bay, 1966 to 1976, Estuaries, 1, 106–110, 1978.

Guido, Z. S., Ward, D. J., and Anderson, R. S.: Pacing the post–Last Glacial Maximum demise of the Animas Valley glacier and the San Juan Mountain ice cap, Colorado, Geology, 35, 739, 2007.

Hager, B. H. and Richards, M. A.: Long-Wavelength Variations in Earth's Geoid: Physical Models and Dynami-
cal Implications, Philosophical Transactions of the Royal Society A: Mathematical, Physical and Engineering
Sciences, 328, 309–327, doi:10.1098/rsta.1989.0038, 1989.

Hanson, M. A., Lian, O. B., and Clague, J. J.: The sequence and timing of large late Pleistocene floods from
glacial Lake Missoula, Quaternary Science Reviews, 31, 67–81, doi:10.1016/j.quascirev.2011.11.009, 2012.

Harmar, O. P. and Clifford, N. J.: Geomorphological explanation of the long profile of the Lower Mississippi
River, Geomorphology, 84, 222–240, doi:10.1016/j.geomorph.2006.01.045, 2007.

Harris, I., Jones, P., Osborn, T., and Lister, D.: Updated high-resolution grids of monthly climatic observations
- the CRU TS3.10 Dataset, International Journal of Climatology, 34, 623–642, doi:10.1002/joc.3711, 2014.

Hay, C., Mitrovica, J. X., Gomez, N., Creveling, J. R., Austermann, J., and Kopp, R. E.: The sea-level
fingerprints of ice-sheet collapse during interglacial periods, Quaternary Science Reviews, 87, 60–69,
doi:10.1016/j.quascirev.2013.12.022, 2014.

He, F.: Simulating Transiet Climate Evolution of the Last Deglaciation with CCSM3, Ph.d. dissertation, Uni-
versity of Wisconsin - Madison, 2011.

Hearty, P. J., Hollin, J. T., Neumann, A. C., O'Leary, M. J., and McCulloch, M.: Global sea-level
fluctuations during the Last Interglaciation (MIS 5e), Quaternary Science Reviews, 26, 2090–2112,
doi:10.1016/j.quascirev.2007.06.019, 2007.

Heinrich, H.: Origin and consequences of cyclic ice rafting in the Northeast Atlantic Ocean during the past
130,000 years, Quaternary Research, 29, 142–152, doi:10.1016/0033-5894(88)90057-9, 1988.

Hemming, S. R.: Heinrich events: Massive late Pleistocene detritus layers of the North Atlantic and their global
climate imprint, Reviews of Geophysics, 42, RG1005, doi:10.1029/2003RG000128, 2004.

Holeman, J. N.: The Sediment Yield of Major Rivers of the World, Water Resources Research, 4, 737–747,
doi:10.1029/WR004i004p00737, 1968.

Huang, P.-c. and Lee, K. T.: An efficient method for DEM-based overland flow routing, Journal of Hydrology,
489, 238–245, doi:10.1016/j.jhydrol.2013.03.014, 2013.

Ivanović, R. F., Gregoire, L. J., Wickert, A. D., and Valdes, P. J.: How did the North American ice Saddle
Collapse impact the climate 14,500 years ago?, in: AGU Fall Meeting Abstracts, American Geophysical
Union, San Francisco, CA, USA, 2014.

John, S., Branch, J. S., Branch, B. C. G. S., Resources, P., Columbia, B., Catto, N., Liverman, D. G. E., Bo-
browsky, P. T., Rutter, N., John, S., Branch, J. S., Branch, B. C. G. S., Resources, P., Columbia, B., Catto, N.,
Liverman, D. G. E., Bobrowsky, P. T., Rutter, N., John, S., Branch, J. S., Branch, B. C. G. S., Resources, P.,
Columbia, B., Catto, N., Liverman, D. G. E., Bobrowsky, P. T., Rutter, N., John, S., Branch, J. S., Branch, B.
C. G. S., Resources, P., Columbia, B., Catto, N., Liverman, D. G. E., Bobrowsky, P. T., and Rutter, N.: Lau-
rentide, cordilleran, and montane glaciation in the western Peace River — Grande Prairie region, Alberta and
British Columbia, Canada, Quaternary International, 32, 21–32, doi:10.1016/1040-6182(95)00061-5, 1996.

Kammerer, J. C.: Largest Rivers in the United States, Open-File Report, United States Geological Survey,
Reston, Virginia, USA., 1990.

Kaufman, D. S. and Miller, G. H.: Abrupt early Holocene (9.9-9.6 ka) ice-stream advance
at the mouth of Hudson Strait, Arctic Canada, Geology, 21, 1063–1066, doi:10.1130/0091-
7613(1993)021<1063:AEHKIS>2.3.CO;2, 1993.

Earth **Surface**
Dynamics
Discussions

Kehew, A. E., Teller, J. T., Tellert, J. T., and Teller, J. T.: History of late glacial runoff along the south-
940   western margin of the Laurentide Ice Sheet, Quaternary Science Reviews, 13, 859–877, doi:10.1016/0277-
3791(94)90006-X, 1994.

Kendall, R. A., Mitrovica, J. X., and Milne, G. A.: On post-glacial sea level–II. Numerical formulation and
comparative results on spherically symmetric models, Geophysical Journal International, 161, 679–706,
doi:10.1111/j.1365-246X.2005.02553.x, 2005.

945   Kettner, A. J. and Syvitski, J. P. M.: HydroTrend v. 3.0: A climate-driven hydrological transport model that
simulates discharge and sediment load leaving a river system, Computers & Geosciences, 34, 1170–1183,
2008.

Kirby, J. F. and Swain, C. J.: A reassessment of spectral T_e estimation in continental interiors: The case of
North America, Journal of Geophysical Research, 114, B08 401, doi:10.1029/2009JB006356, 2009.

950   Knox, J. C.: The Mississippi River System, in: Large rivers: geomorphology and management, edited by Gupta,
A., pp. 145–182, Wiley, 2007.

Kutzbach, J. E. and Wright, H. E.: Simulation of the climate of 18,000 years BP: Results for the North Ameri-
can/North Atlantic/European sector and comparison with the geologic record of North America, Quaternary
Science Reviews, 4, 147–187, doi:10.1016/0277-3791(85)90024-1, 1985.

955   Lambeck, K., Yokoyama, Y., and Purcell, T.: Into and out of the Last Glacial Maximum: sea-level change during
Oxygen Isotope Stages 3 and 2, Quaternary Science Reviews, 21, 343–360, 2002.

Lambeck, K., Rouby, H., Purcell, A., Sun, Y., and Sambridge, M.: Sea level and global ice volumes
from the Last Glacial Maximum to the Holocene, Proceedings of the National Academy of Sciences,
doi:10.1073/pnas.1411762111, 2014.

960   Lavoie, C., Allard, M., and Duhamel, D.: Deglaciation landforms and C-14 chronology of the Lac Guillaume-
Delisle area, eastern Hudson Bay: A report on field evidence, Geomorphology, 159-160, 142–155,
doi:10.1016/j.geomorph.2012.03.015, 2012.

Lehner, B., Verdin, K., and Jarvis, A.: HydroSHEDS Technical Documentation Version 1.2, vol. 89, 2013.

Lemieux, J.-M., Sudicky, E. A., Peltier, W. R., and Tarasov, L.: Dynamics of groundwater recharge and seepage
965   over the Canadian landscape during the Wisconsinian glaciation, Journal of Geophysical Research, 113,
1–18, doi:10.1029/2007JF000838, 2008.

Lemmen, D. S. D. D. S., Duk-Rodkin, A., and Bednarski, J. M. A. N. M.: Late glacial drainage systems along
the northwestern margin of the Laurentide Ice Sheet, Quaternary Science Reviews, 13, 805–828, 1994.

Leopold, L. B. and Maddock, T.: The hydraulic geometry of stream channels and some physiographic implica-
970   tions, Professional Paper, United States Geological Survey, Washington, D.C., 1953.

Lewis, C. F. M. and Teller, J. T.: Glacial runoff from North America and its possible impact on
oceans and climate, in: Glacier Science and Environmental Change, chap. Chapter Tw, pp. 138–150,
doi:10.1002/9780470750636.ch28, 2006.

Licciardi, J. M., Teller, J. T., and Clark, P. U.: Freshwater routing by the Laurentide Ice Sheet during the last
975   deglaciation, in: Mechanisms of global climate change at millennial time scales, vol. 112, pp. 177–201, 1999.

Liu, Z., Otto-Bliesner, B. L., He, F., Brady, E. C., Tomas, R., Clark, P. U., Carlson, A. E., Lynch-Stieglitz,
J., Curry, W., Brook, E., Erickson, D., Jacob, R., Kutzbach, J., and Cheng, J.: Transient simulation of last

deglaciation with a new mechanism for Bolling-Allerod warming., Science (New York, N.Y.), 325, 310–314, doi:10.1126/science.1171041, 2009.

980   Livingstone, S. J., Storrar, R. D., Hillier, J. K., Stokes, C. R., Clark, C. D., and Tarasov, L.: An ice-sheet scale comparison of eskers with modelled subglacial drainage routes, Geomorphology, 246, 104–112, doi:10.1016/j.geomorph.2015.06.016, 2015.

Lowell, T. V., Applegate, P. J., Fisher, T. G., and Lepper, K.: What caused the low-water phase of glacial Lake Agassiz?, Quaternary Research, 80, 370–382, doi:10.1016/j.yqres.2013.06.002, 2013.

985   MacAyeal, D. R.: Binge/purge oscillations of the Laurentide Ice Sheet as a cause of the North Atlantic's Heinrich events, Paleoceanography, 8, 775, doi:10.1029/93PA02200, 1993.

Maccali, J., Hillaire-Marcel, C., Carignan, J., and Reisberg, L. C.: Geochemical signatures of sediments documenting Arctic sea-ice and water mass export through Fram Strait since the Last Glacial Maximum, Quaternary Science Reviews, 64, 136–151, doi:10.1016/j.quascirev.2012.10.029, 2013.

990   Mackay, J. R. and Mathews, W. H.: Geomorphology and Quaternary History of the Mackenzie River Valley near Fort Good Hope, N.W.T., Canada, Canadian Journal of Earth Sciences, 10, 26–41, doi:10.1139/e73-003, 1973.

Margold, M., Stokes, C. R., Clark, C. D., and Kleman, J.: Ice streams in the Laurentide Ice Sheet : a new mapping inventory, Journal of Maps, 16, 9669, doi:10.1080/17445647.2014.912036, 2014.

995   Margold, M., Stokes, C. R., and Clark, C. D.: Ice streams in the Laurentide Ice Sheet: Identification, characteristics and comparison to modern ice sheets, Earth-Science Reviews, 143, 117–146, doi:10.1016/j.earscirev.2015.01.011, 2015.

Marshall, S. J. and Clarke, G. K. C.: Modeling North American freshwater runoff through the last glacial cycle, Quaternary Research, 52, 300–315, 1999.

1000 Matsubara, Y. and Howard, A. D.: A spatially explicit model of runoff, evaporation, and lake extent: Application to modern and late Pleistocene lakes in the Great Basin region, western United States, Water Resources Research, 45, W06 425, doi:10.1029/2007WR005953, 2009.

McGee, D., Quade, J., Edwards, R. L., Broecker, W. S., Cheng, H., Reiners, P. W., and Evenson, N.: Lacustrine cave carbonates: Novel archives of paleohydrologic change in the Bonneville Basin (Utah, USA), Earth and
1005 Planetary Science Letters, 351-352, 182–194, doi:10.1016/j.epsl.2012.07.019, 2012.

Metz, J. M., Dowdeswell, J., and Woodworth-Lynas, C. M. T.: Sea-floor scour at the mouth of Hudson Strait by deep-keeled icebergs from the Laurentide Ice Sheet, Marine Geology, 253, 149–159, doi:10.1016/j.margeo.2008.05.004, 2008.

Metz, M., Mitasova, H., and Harmon, R. S.: Efficient extraction of drainage networks from massive, radar-
1010 based elevation models with least cost path search, Hydrology and Earth System Sciences, 15, 667–678, doi:10.5194/hess-15-667-2011, 2011.

Milliman, J. and Farnsworth, K.: River discharge to the coastal ocean: a global synthesis, Cambridge University Press, 2013.

Milliman, J. D. and Meade, R. H.: World-wide delivery of river sediment to the oceans, The Journal of Geology,
1015 91, 1–21, 1983.

Mitrovica, J. X.: Haskell [1935] revisited, Journal of Geophysical Research, 101, 555–569, doi:10.1029/95JB03208, 1996.

Mitrovica, J. X. and Milne, G. A.: On post-glacial sea level: I. General theory, Geophysical Journal International, 154, 253–267, doi:10.1046/j.1365-246X.2003.01942.x, 2003.

1020   Monteleone, K., Dixon, E. J., and Wickert, A. D.: Lost Worlds: A predictive model to locate submerged archaeological sites in SE Alaska, USA, in: Archaeology in the Digital Era: Papers from the 40th Annual Conference of Computer Applications and Quantitative Methods in Archaeology (CAA), Southampton, 26-29 March 2012, edited by Earl, G., Sly, T., Chrysanthi, A., Murrieta-Flores, P., Papadopoulos, C., Romanowska, I., and Wheatley, D., pp. 1–12, Amsterdam University Press, Southampton, UK, 2013.

1025   Monteleone, K. R.: Lost worlds: Locating submerged archaeological sites in Southeast Alaska, Ph.d. dissertation, The University of New Mexico, 2013.

Montero-Serrano, J. C., Bout-Roumazeilles, V., Tribovillard, N., Sionneau, T., Riboulleau, A., Bory, A., and Flower, B.: Sedimentary evidence of deglacial megafloods in the northern Gulf of Mexico (Pigmy Basin), Quaternary Science Reviews, 28, 3333–3347, doi:10.1016/j.quascirev.2009.09.011, 2009.

1030   Mu, Q., Heinsch, F. A., Zhao, M., and Running, S. W.: Development of a global evapotranspiration algorithm based on MODIS and global meteorology data, Remote Sensing of Environment, 111, 519–536, doi:10.1016/j.rse.2007.04.015, 2007.

Mu, Q., Zhao, M., and Running, S. W.: Improvements to a MODIS global terrestrial evapotranspiration algorithm, Remote Sensing of Environment, 115, 1781–1800, doi:10.1016/j.rse.2011.02.019, 2011.

1035   Murton, J. B., Bateman, M. D., Dallimore, S. R., Teller, J. T., and Yang, Z.: Identification of Younger Dryas outburst flood path from Lake Agassiz to the Arctic Ocean., Nature, 464, 740–743, doi:10.1038/nature08954, 2010.

Neteler, M., Bowman, M. H., Landa, M., and Metz, M.: GRASS GIS: A multi-purpose open source GIS, Environmental Modelling & Software, 31, 124–130, doi:10.1016/j.envsoft.2011.11.014, 2012.

1040   Nowak, K. C.: Stochastic streamflow simulation at interdecadal time scales and implications to water resources management in the Colorado River Basin, Ph.d. thesis, University of Colorado, 2011.

Occhietti, S., Govare, E., Klassen, R., Parent, M., and Vincent, J.-S.: Late Wisconsinan–Early Holocene deglaciation of Québec-Labrador, in: Quaternary Glaciations – Extent and Chronology — Part II: North America, edited by Ehlers, J. and Gibbard, P. L., Developments in Quaternary Sciences, pp. 243–273, 2004.

1045   Ó Cofaigh, C., Evans, D. J. A., and Smith, I. R.: Large-scale reorganization and sedimentation of terrestrial ice streams during late Wisconsinan Laurentide Ice Sheet deglaciation, Geological Society of America Bulletin, 122, 743–756, doi:10.1130/B26476.1, 2010.

Orme, A. R.: Pleistocene pluvial lakes of the American West: a short history of research, Geological Society, London, Special Publications, 301, 51–78, doi:10.1144/SP301.4, 2008.

1050   Overeem, I., Syvitski, J. P. M., Hutton, E. W. H., and Kettner, A. J.: Stratigraphic variability due to uncertainty in model boundary conditions: A case-study of the New Jersey Shelf over the last 40,000 years, Marine Geology, 224, 23–41, 2005.

Owen, L. A., Finkel, R. C., Minnich, R. A., and Perez, A. E.: Extreme southwestern margin of late Quaternary glaciation in North America: Timing and controls, Geology, 31, 729, doi:10.1130/G19561.1, 2003.

1055   Patterson, C. J.: Southern Laurentide ice lobes were created by ice streams: Des Moines Lobe in Minnesota, USA, Sedimentary Geology, 111, 249–261, doi:10.1016/S0037-0738(97)00018-3, 1997.

Patterson, C. J.: Laurentide glacial landscapes: The role of ice streams, Geology, 26, 643, doi:10.1130/0091-7613(1998)026<0643:LGLTRO>2.3.CO;2, 1998.

Pelletier, J. D.: A spatially distributed model for the long-term suspended sediment discharge and delivery ratio of drainage basins, Journal of Geophysical Research, 117, F02 028, doi:10.1029/2011JF002129, 2012.

Peltier, W. R., Argus, D. F., and Drummond, R.: Space geodesy constrains ice age terminal deglaciation: The global ICE-6G_C (VM5a)model, Journal of Geophysical Research: Solid Earth, 120, 450–487, doi:10.1002/2014JB011176, 2015.

Peltier, W. R. R.: Global Glacial Isostasy and the Surface of the Ice-Age Earth: The ICE-5G (VM2) Model and GRACE, Annual Review of Earth and Planetary Sciences, 32, 111–149, doi:10.1146/annurev.earth.32.082503.144359, 2004.

Polyak, V. J., Rasmussen, J. B. T., and Asmerom, Y.: Prolonged wet period in the southwestern United States through the Younger Dryas, Geology, 32, 5, doi:10.1130/G19957.1, 2004.

Prairie, J. and Callejo, R.: Natural Flow And Salt Computation Methods: Calendar Years 1971-1995, December, U.S. Department of the Interior, Bureau of Reclamation, Salt Lake City, UT, and Boulder City, NV, 2005.

Prince, P. S. and Spotila, J. A.: Evidence of transient topographic disequilibrium in a landward passive margin river system: knickpoints and paleo-landscapes of the New River basin, southern Appalachians, Earth Surface Processes and Landforms, 38, 1685–1699, doi:10.1002/esp.3406, 2013.

Qin, C.-z. and Zhan, L.: Parallelizing flow-accumulation calculations on graphics processing units—From iterative DEM preprocessing algorithm to recursive multiple-flow-direction algorithm, Computers & Geosciences, 43, 7–16, doi:10.1016/j.cageo.2012.02.022, 2012.

Rashid, H., Hesse, R., and Piper, D. J. W.: Origin of unusually thick Heinrich layers in ice-proximal regions of the northwest Labrador Sea, Earth and Planetary Science Letters, 208, 319–336, doi:10.1016/S0012-821X(03)00030-X, 2003.

Rayburn, J. A., K. Knuepfer, P. L., and Franzi, D. A.: A series of large, Late Wisconsinan meltwater floods through the Champlain and Hudson Valleys, New York State, USA, Quaternary Science Reviews, 24, 2410–2419, doi:10.1016/j.quascirev.2005.02.010, 2005.

Rayburn, J. A., Franzi, D. A., and Knuepfer, P. L. K.: Evidence from the Lake Champlain Valley for a later onset of the Champlain Sea and implications for late glacial meltwater routing to the North Atlantic, Palaeogeography, Palaeoclimatology, Palaeoecology, 246, 62–74, doi:10.1016/j.palaeo.2006.10.027, 2007.

Rayburn, J. A., Cronin, T. M., Franzi, D. A., Knuepfer, P. L. K., and Willard, D. A.: Timing and duration of North American glacial lake discharges and the Younger Dryas climate reversal, Quaternary Research, 75, 541–551, doi:10.1016/j.yqres.2011.02.004, 2011.

Reimer, P. J., Bard, E., Bayliss, A., Beck, J. W., Blackwell, P. G., Ramsey, C. B., Grootes, P. M., Guilderson, T. P., Haflidason, H., Hajdas, I., Hatté, C., Heaton, T. J., Hoffmann, D. L., Hogg, A. G., Hughen, K. A., Kaiser, K. F., Kromer, B., Manning, S. W., Niu, M., Reimer, R. W., Richards, D. A., Scott, E. M., Southon, J. R., Staff, R. A., Turney, C. S. M., van der Plicht, J., and van der Plicht, J.: IntCal13 and Marine13 Radiocarbon Age Calibration Curves 0–50,000 Years cal BP, Radiocarbon, 55, 1869–1887, doi:10.2458/azu_js_rc.55.16947, 2013.

1095   Reneau, S. L. and Dethier, D. P.: Late Pleistocene landslide-dammed lakes along the Rio Grande, White
          Rock Canyon, New Mexico, Geological Society of America Bulletin, 108, 1492–1507, doi:10.1130/0016-
          7606(1996)108<1492:LPLDLA>2.3.CO;2, 1996.

       Reusser, L., Bierman, P., Pavich, M., Larsen, J., and Finkel, R.: An episode of rapid bedrock channel in-
          cision during the last glacial cycle, measured with 10Be, American Journal of Science, 306, 69–102,
1100   doi:10.2475/ajs.306.2.69, 2006.

       Richard, P. J. H., Occhietti, S., T, P. J. H. R., Occhietti, S., Richard, P. J. H., and Occhietti, S.: 14C chronology
          for ice retreat and inception of Champlain Sea in the St. Lawrence Lowlands, Canada, Quaternary Research,
          63, 353–358, doi:10.1016/j.yqres.2005.02.003, 2005.

       Ridge, J. C.: Shed Brook Discontinuity and Little Falls Gravel: Evidence for the Erie interstade
1105   in central New York, Geological Society of America Bulletin, 109, 652–665, doi:10.1130/0016-
          7606(1997)109<0652:SBDALF>2.3.CO;2, 1997.

       Ridge, J. C., Franzi, D. A., and Muller, E. H.: Late Wisconsinan, pre-Valley Heads glaciation in the western
          Mohawk Valley, central New York, and its regional implications, Geological Society of America Bulletin,
          103, 1032–1048, doi:10.1130/0016-7606(1991)103<1032:LWPVHG>2.3.CO;2, 1991.

1110   Rittenour, T. M., Blum, M. D., and Goble, R. J.: Fluvial evolution of the lower Mississippi River valley during
          the last 100 ky glacial cycle: Response to glaciation and sea-level change, Bulletin of the Geological Society
          of America, 119, 586, 2007.

       Roberts, G. G., White, N. J., Martin-Brandis, G. L., and Crosby, a. G.: An uplift history of the Colorado
          Plateau and its surroundings from inverse modeling of longitudinal river profiles, Tectonics, 31, 1–2,
1115   doi:10.1029/2012TC003107, 2012.

       Rohling, E. J., Grant, K., Hemleben, C., Siddall, M., Hoogakker, B. a. a., Bolshaw, M., and Kucera,
          M.: High rates of sea-level rise during the last interglacial period, Nature Geoscience, 1, 38–42,
          doi:10.1038/ngeo.2007.28, 2007.

       Ross, M., Campbell, J. E., Parent, M., and Adams, R. S.: Palaeo-ice streams and the subglacial land-
1120   scape mosaic of the North American mid-continental prairies, Boreas, 38, 421–439, doi:10.1111/j.1502-
          3885.2009.00082.x, 2009.

       Rutt, I. C., Hagdorn, M., Hulton, N. R. J., and Payne, a. J.: The Glimmer community ice sheet model, Journal
          of Geophysical Research, 114, F02 004, doi:10.1029/2008JF001015, 2009.

       Schmidt, J. C., Schmidt, B. J. C., and Schmidt, J. C.: A Watershed Perspective of Changes in Streamflow ,
1125   Sediment Supply , and Geomorphology of the Colorado River, in: Proceedings of the Colorado River Basin
          Science and Resource Management Symposium, November 18–20, 2008, Scottsdale, Arizona, edited by
          Melis, T. S., Hamill, J. F., Bennett, G. E., Lewis G. Coggins, J., Grams, P. E., Kennedy, T. A., Kubly, D. M.,
          and Ralston, B. E., vol. 2009 of *USGS Scientific Investigations Report*, pp. 51–76, United States Geological
          Survey, Scottsdale, Arizona, USA, 2010.

1130   Schneider-Vieira, F., Baker, R., and Lawrence, M.: The Estuaries of Hudson Bay: A Case Study of the Physical
          and Biological Characteristics of Selected Sites, North/South Consultants Inc., Winnipeg, Manitoba, Canada,
          1994.

Schwanghart, W. and Scherler, D.: Short Communication: TopoToolbox 2 – MATLAB-based software for topographic analysis and modeling in Earth surface sciences, Earth Surface Dynamics, 2, 1–7, doi:10.5194/esurf-2-1-2014, 2014.

Sionneau, T., Bout-Roumazeilles, V., Biscaye, P., Van Vliet-Lanoe, B., and Bory, A.: Clay mineral distributions in and around the Mississippi River watershed and Northern Gulf of Mexico: sources and transport patterns, Quaternary Science Reviews, 27, 1740–1751, doi:10.1016/j.quascirev.2008.07.001, 2008.

Sionneau, T., Bout-Roumazeilles, V., Flower, B. P., Bory, A., Tribovillard, N., Kissel, C., Van Vliet-Lanoë, B., and Montero Serrano, J. C.: Provenance of freshwater pulses in the Gulf of Mexico during the last deglaciation, Quaternary Research, 74, 235–245, doi:10.1016/j.yqres.2010.07.002, 2010.

Stokes, C. R., Clark, C. D., and Storrar, R.: Major changes in ice stream dynamics during deglaciation of the north-western margin of the Laurentide Ice Sheet, Quaternary Science Reviews, 28, 721–738, doi:10.1016/j.quascirev.2008.07.019, 2009.

Storrar, R. D., Stokes, C. R., and Evans, D. J.: A map of large Canadian eskers from Landsat satellite imagery, Journal of Maps, 9, 456–473, doi:10.1080/17445647.2013.815591, 2013.

Stroup, J. S., Lowell, T. V., and Breckenridge, A.: A model for the demise of large, glacial Lake Ojibway, Ontario and Quebec, Journal of Paleolimnology, 50, 105–121, 2013.

Svensson, A., Andersen, K. K., Bigler, M., Clausen, H. B., Dahl-Jensen, D., Davies, S. M., Johnsen, S. J., Muscheler, R., Parrenin, F., Rasmussen, S. O., Röthlisberger, R., Seierstad, I., Steffensen, J. P., and Vinther, B. M.: A 60 000 year Greenland stratigraphic ice core chronology, Climate of the Past, 4, 47–57, doi:10.5194/cp-4-47-2008, 2008.

Syvitski, J. P. M., Peckham, S. D., Hilberman, R., and Mulder, T.: Predicting the terrestrial flux of sediment to the global ocean: a planetary perspective, Sedimentary Geology, 162, 5–24, doi:10.1016/S0037-0738(03)00232-X, 2003.

Tarasov, L. and Peltier, W. R.: Arctic freshwater forcing of the Younger Dryas cold reversal., Nature, 435, 662–665, doi:10.1038/nature03617, 2005.

Tarasov, L. and Peltier, W. R. R.: A calibrated deglacial drainage chronology for the North American continent: evidence of an Arctic trigger for the Younger Dryas, Quaternary Science Reviews, 25, 659–688, doi:10.1016/j.quascirev.2005.12.006, 2006.

Tarasov, L., Dyke, A. S., Neal, R. M., and Peltier, W. R.: A data-calibrated distribution of deglacial chronologies for the North American ice complex from glaciological modeling, Earth and Planetary Science Letters, 315-316, 30–40, doi:10.1016/j.epsl.2011.09.010, 2012.

Taylor, M., Hendy, I., and Pak, D.: Deglacial ocean warming and marine margin retreat of the Cordilleran Ice Sheet in the North Pacific Ocean, Earth and Planetary Science Letters, 403, 89–98, doi:10.1016/j.epsl.2014.06.026, 2014.

Teller, J. T.: Preglacial (Teays) and Early Glacial Drainage in the Cincinnati Area, Ohio, Kentucky, and Indiana, Geological Society of America Bulletin, 84, 3677, doi:10.1130/0016-7606(1973)84<3677:PTAEGD>2.0.CO;2, 1973.

Teller, J. T.: Meltwater and precipitation runoff to the North Atlantic, Arctic, and Gulf of Mexico from the Laurentide Ice Sheet and adjacent regions during the Younger Dryas, Paleoceanography, 5, 897–905, doi:10.1029/PA005i006p00897, 1990a.

Teller, J. T. and Leverington, D. W.: Glacial Lake Agassiz: A 5000 yr history of change and its relationship to the δ18O record of Greenland, Geological Society of America Bulletin, 116, 729, doi:10.1130/B25316.1, 2004.

Teller, J. T., Leverington, D. W., and Mann, J. D.: Freshwater outbursts to the oceans from glacial Lake Agassiz and their role in climate change during the last deglaciation, Quaternary Science Reviews, 21, 879–887, doi:10.1016/S0277-3791(01)00145-7, 2002.

Teller, J. T. J. T.: Volume and routing of late-glacial runoff from the southern Laurentide Ice Sheet, Quaternary Research, 34, 12–23, doi:10.1016/0033-5894(90)90069-W, 1990b.

Tesauro, M., Kaban, M. K., and Cloetingh, S. A. P. L.: Global strength and elastic thickness of the lithosphere, Global and Planetary Change, 90-91, 51–57, doi:10.1016/j.gloplacha.2011.12.003, 2012.

Tight, W. G.: Drainage modifications in southeastern Ohio and adjacent parts of West Virginia and Kentucky, US Geological Survey Professional Paper, US Geological Survey, Reston, Virginia, USA., 1903.

Tripsanas, E. K., Bryant, W. R., Slowey, N. C., Bouma, A. H., Karageorgis, A. P., and Berti, D.: Sedimentological history of Bryant Canyon area, northwest Gulf of Mexico, during the last 135 kyr (Marine Isotope Stages 1–6): A proxy record of Mississippi River discharge, Palaeogeography, Palaeoclimatology, Palaeoecology, 246, 137–161, doi:10.1016/j.palaeo.2006.10.032, 2007.

Tucker, G. E. and Whipple, K. X.: Topographic outcomes predicted by stream erosion models: Sensitivity analysis and intermodel comparison, Journal of Geophysical Research, 107, 1–16, doi:10.1029/2001JB000162, 2002.

Tushingham, A. M. and Peltier, W. R.: Ice-3G: A new global model of Late Pleistocene deglaciation based upon geophysical predictions of post-glacial relative sea level change, Journal of Geophysical Research, 96, 4497, doi:10.1029/90JB01583, 1991.

Ullman, D. J., LeGrande, A. N., Carlson, A. E., Anslow, F. S., and Licciardi, J. M.: Assessing the impact of Laurentide Ice Sheet topography on glacial climate, Climate of the Past, 10, 487–507, doi:10.5194/cp-10-487-2014, 2014.

U.S. Bureau of Reclamation: Report on the Water Supply of the Lower Colorado River, Project Planning Report, 1952.

van Andel, T. H.: Recent marine sediments of the Gulf of California, in: Marine Geology of the Gulf of California: A Symposium, edited by van Andel, T. J. and Shor, G. G., Memoir, pp. 216–310, American Association of Petroleum Geologists, 1964.

van Hise, C. R. and Leith, C. K.: The geology of the Lake Superior region, Monographs, United States Geological Survey, Washington, D.C., 1911.

Ver Steeg, K.: The Teays River, The Ohio Journal of Science, 46, 297–307, 1946.

Wagner, J. D. M., Cole, J. E., Beck, J. W., Patchett, P. J., Henderson, G. M., and Barnett, H. R.: Moisture variability in the southwestern United States linked to abrupt glacial climate change, Nature Geoscience, 3, 110–113, doi:10.1038/ngeo707, 2010.

Waitt, R. B. J.: About forty last-glacial Lake Missoula jökulhlaups through southern Washington, The Journal of Geology, 88, 653–679, 1980.

Wall, G. R., Nystrom, E. a., and Litten, S.: Suspended Sediment Transport in the Freshwater Reach of the Hudson River Estuary in Eastern New York, Estuaries and Coasts, 31, 542–553, doi:10.1007/s12237-008-9050-y, 2008.

Wickert, A. D.: Impacts of Pleistocene glaciation and its geophysical effects on North American river systems, Ph.d. dissertation, University of Colorado Boulder, 2014.

Wickert, A. D., Mitrovica, J. X., Williams, C., and Anderson, R. S.: Gradual demise of a thin southern Laurentide ice sheet recorded by Mississippi drainage, Nature, 502, 668–671, doi:10.1038/nature12609, 2013.

Willgoose, G.: Mathematical Modeling of Whole Landscape Evolution, Annual Review of Earth and Planetary Sciences, 33, 443–459, doi:10.1146/annurev.earth.33.092203.122610, 2005.

Williams, C., Flower, B. P., Hastings, D. W., Guilderson, T. P., Quinn, K. A., and Goddard, E. A.: Deglacial abrupt climate change in the Atlantic Warm Pool: A Gulf of Mexico perspective, Paleoceanography, 25, PA4221, doi:10.1029/2010PA001928, 2010.

Williams, C., Flower, B. P., and Hastings, D. W.: Seasonal Laurentide Ice Sheet melting during the "Mystery Interval" (17.5-14.5 ka), Geology, 40, 955–958, doi:10.1130/G33279.1, 2012.

Wright, H.: Tunnel valleys, glacial surges, and subglacial hydrology of the Superior Lobe, Minnesota, Geological Society of America Memoir, 136, 251–276, 1973.

Wright, H. E. J.: Synthesis: the land south of the ice sheets, in: North America and Adjacent Oceans During the Last Deglaciation, edited by Ruddiman, W. F. and Wright, H. E. J., Geology of North America, pp. 479–488, Geological Society of America, Boulder, Colorado, USA, 1987.

Xie, P. and Arkin, P. A.: Global Precipitation: A 17-Year Monthly Analysis Based on Gauge Observations, Satellite Estimates, and Numerical Model Outputs, Bulletin of the American Meteorological Society, 78, 2539–2558, doi:10.1175/1520-0477(1997)078<2539:GPAYMA>2.0.CO;2, 1997.

Yeager, S. G., Shields, C. A., Large, W. G., and Hack, J. J.: The low-resolution CCSM3, Journal of Climate, 19, 2545–2566, doi:10.1175/JCLI3744.1, 2006.

Zuffa, G., Normark, W., Serra, F., and Brunner, C.: Turbidite megabeds in an oceanic rift valley recording jökulhlaups of late Pleistocene glacial lakes of the western United States, The Journal of Geology, 108, 253–274, 2000.